Table 1. Evaluation of Body Weight, Biliary Expression of SR, Lobular Necrosis, Percentage of PCNA- or TUNEL-Positive Large Cholangiocytes, and Large IBDM in Liver Sections

Groups	Body Weight (g)	Percentage of Large Cholangiocytes Positive for SR	Lobular Necrosis	Percentage of Large Cholangiocytes Positive for PCNA	Large IBDM	Percentage of Large Cholangiocytes Positive by TUNEL
WT normal + NaCl, 1 week	27.8 ± 0.8	19.83 ± 1.96	(−)	6.20 ± 0.97	0.17 ± 0.03	ND
WT normal + secretin, 1 week	25.6 ± 0.5	30.60 ± 2.04*	(−)	40.80 ± 2.29*	0.35 ± 0.02*	ND
Normal $SR^{-/-}$ + NaCl, 1 week	28.6 ± 0.7	ND	(−)	4.20 ± 0.66	0.18 ± 0.02	ND
Normal $SR^{-/-}$ + secretin, 1 week	29.0 ± 1.8	ND	(−)	5.33 ± 1.08	0.18 ± 0.03	ND
WT BDL, 3 days	23.2 ± 0.7	39.0 ± 2.07*	(+)	60.62 ± 2.30	1.26 ± 0.06	ND
$SR^{-/-}$ BDL, 3 days	22.0 ± 0.5	ND	(++)	39.67 ± 2.16†	0.57 ± 0.06†	10.50 ± 1.08
WT BDL, 7 days	23.2 ± 0.7	41.33 ± 2.35*	(+)	47.67 ± 1.50	2.51 ± 0.12	ND
$SR^{-/-}$ BDL, 7 days	26.2 ± 0.6	ND	(++)	30.83 ± 2.07†	1.40 ± 0.11†	13.33 ± 0.88

Body weight values are derived from 10-20 animals per each group. Evaluations were performed in liver sections (4- to 5-μm-thick). IBDM was measured as the area occupied by cytokeratin-19-positive bile duct/total area x 100. Lobular necrosis was scored as follows: −, 0 foci; +/−, <2 foci; +, 2-4 foci; ++, >4 foci. Data are expressed as the mean ± SEM.

Abbreviations: ND, not detected; TUNEL, terminal deoxynucleotidyl transferase-mediated dUTP nick-end labeling.

*$P < 0.05$ versus the corresponding value of WT normal mice treated with NaCl for 1 week.

†$P < 0.05$ versus the corresponding value of WT mice with BDL for 3 and 7 days, respectively.

days; or (2) for sham operation or BDL (for 3 and 7 days).[5,20,22] Because our previous studies[21] showed that $SR^{-/-}$ mice have a renal defect in water reabsorption and associated polyuria and polydipsia, experiments were performed to determine whether the response of $SR^{-/-}$ mice to BDL was due to the lack of SR rather than severe dehydration. Thus, we evaluated changes in body weight and mortality rate in the experimental groups of Table 1. In addition, both WT and $SR^{-/-}$ mice (after BDL or administration of secretin) received oral hydration therapy, consisting of up to 1 ml of normal saline subcutaneously up to twice daily along with water in gel form on the ground and food supplements. Because there were no differences in cholangiocyte proliferation between normal WT and normal $SR^{-/-}$ mice and their corresponding sham mice, we did not show the results from the sham animals.

Immortalized and Freshly Isolated Cholangiocytes. The *in vitro* studies were performed in freshly isolated or immortalized[5,8] large cholangiocytes. The rationale for performing these studies only in large cholangiocytes is based on the fact that secretin stimulated *in vivo* the proliferation of only large bile ducts and that following BDL, large but not small cholangiocytes proliferate.[5] Freshly isolated large cholangiocytes (≈99% by cytokeratin-19 immunohistochemistry)[5,20] were purified by centrifugal elutriation[4,9,14] followed by immunoaffinity separation by a monoclonal antibody, rat IgG_{2a} (provided by Dr. R. Faris, Brown University, Providence, RI), against an antigen expressed by all mouse cholangiocytes.[5] Our large mouse cholangiocyte lines, which display morphological, phenotypic, and functional features similar to that of freshly isolated large cholangiocytes were cultured as described.[5,8,9]

Evaluation of Secretin Receptor Expression. We evaluated the expression of SR by immunohistochemistry in paraffin-embedded liver sections from the experimental groups of Table 1. Because immunohistochemistry shows that only large bile ducts from WT (but not knockout) animals express SR, we evaluated the expression of SR by way of immunofluorescence and real-time polymerase chain reaction (PCR) in freshly isolated large cholangiocytes from normal and 3- and 7-day BDL WT mice. Semiquantitative immunohistochemical analysis of SR expression in sections was performed as described.[5] Light microscopy photographs of liver sections were taken by Leica Microsystems DM 4500 B Light Microscopy (Weltzlar, Germany) with a Jenoptik Prog Res C10 Plus Videocam (Jena, Germany). Immunofluorescence for SR was also performed in large cholangiocytes from normal and 3- and 7-day BDL WT mice.[5,20] Images were visualized using an Olympus IX-71 confocal microscope. For all immunoreactions, negative controls (with normal serum from the same species substituted for the primary antibody) were included.

In freshly isolated large cholangiocytes from normal and BDL WT mice, messenger RNA and protein expression of SR were evaluated by way of real-time PCR[23] and western blot analysis, respectively.[20] For real-time PCR, RNA was extracted from cholangiocytes using the RNeasy Mini Kit (Qiagen Inc, Valencia, CA) and reverse-transcribed using the Reaction Ready First Strand cDNA synthesis kit (SuperArray, Frederick, MD). These reactions were used as templates for the PCR assays using an SYBR Green PCR

master mix and specific primers designed against the mouse secretin receptor gene NM_001012322,[24] and glyceraldehyde 3-phosphate dehydrogenase, the housekeeping gene (SuperArray, Frederick, MD) in the real-time thermal cycler (ABI Prism 7900HT sequence detection system). A ΔΔCt analysis was performed using normal large cholangiocytes as the control sample. Data are expressed as fold-change of relative messenger RNA levels ± standard error of the mean (SEM) (n = 6).

Evaluation of Liver Histology, Cholangiocyte Apoptosis, and Proliferation. All liver sections were scored by two board-certified pathologists who were blinded to the identity of the samples. Lobular necrosis was evaluated in liver sections stained with hematoxylin-eosin.[25] Lobular necrosis was scored as follows: −, 0 foci; +/−, <2 foci; +, 2-4 foci; ++, >4 foci.[25] Sections were examined in a coded fashion by BX-51 light microscopy (Olympus, Tokyo, Japan) equipped with a camera. We measured (1) the percentage of cholangiocyte apoptosis by semiquantitative terminal deoxynucleotidyl transferase–mediated dUTP nick-end labeling kit (Apoptag; Chemicon International, Inc.); (2) cholangiocyte proliferation by evaluation of the percentage of small and large cholangiocytes positive for PCNA[5]; and (3) intrahepatic bile duct mass (IBDM)[5] of small (<15 μm)[1] and large (>15 μm)[1] bile ducts. IBDM was measured as the area occupied by cytokeratin-19–positive bile duct/total area × 100. Proliferation was evaluated by immunoblots[20] for PCNA in protein (10 μg) from lysate from spleen (positive control) and large cholangiocytes from WT and $SR^{-/-}$ BDL mice. Blots were normalized by β-actin.[5] The intensity of the bands was determined by way of scanning video densitometry using the Storm 860 and the ImageQuant TL software version 2003.02 (GE Healthcare, Little Chalfont, Buckinghamshire, England).

Measurement of cAMP Levels and Phosphorylation of ERK1/2. These experiments were performed in large cholangiocytes from WT and knockout 7-day BDL mice, a period where a marked ductal hyperplasia is observed.[2,12] We evaluated basal and secretin-stimulated cAMP levels (a functional parameter of cholangiocyte growth)[13,18] by commercially available RIA kits[20]; and phosphorylation of ERK1/2 by immunoblots in protein (10 μg) from cholangiocyte lysate. The intensities of the bands were determined by scanning video densitometry using a phospho-imager.

***In Vitro* Effect of Secretin on the Proliferation, Protein Kinase A Activity, and ERK1/2 Phosphorylation of Large Cholangiocytes.** Our small (negative control) and large cholangiocytes[8] were treated at 37°C with 0.2% bovine serum albumin (BSA) (basal) or secretin (100 nM) for 48 hours in the absence or presence of preincubation (1 hour) with H89 (protein kinase A [PKA] inhibitor, 30 μM) or PD98059 (mitogen-activated protein kinase kinase [MEK] inhibitor, 10 nM) before evaluating proliferation by CellTiter 96 Cell Proliferation Assay[20] (Promega Corp., Madison, WI). Absorbance was measured at 490 nm on a microplate spectrophotometer (Molecular Devices, Sunnyvale, CA). Data were expressed as the fold change of treated cells compared with vehicle-treated controls. In separate experiments, large cholangiocytes were treated with 0.2% BSA (basal) or secretin (100 nM) for 6 hours in the absence or presence of H89 (30 μM) or PD98059 (10 nM) before evaluating PCNA expression by way of immunoblotting,[5] PKA activity,[20] and phosphorylation of ERK1/2 by way of immunoblotting.[5] The intensity of the bands was determined as described above.

Stable Transfected Knockdown of Secretin Receptor in Large Cholangiocytes. To provide conclusive evidence that SR is a key proproliferative regulator sustaining large cholangiocyte growth, we stably knocked down the expression of this receptor in large cholangiocyte lines.[8] The mouse cell line lacking SR was established using SureSilencing short hairpin RNA (SuperArray, Frederick, MD) plasmid for mouse SR containing a marker for neomycin resistance for the selection of stably transfected cells, according to the instructions provided by the vendor as described.[23] A total of four clones were assessed for the relative knockdown of the SR gene using real-time PCR and a single clone with the greatest degree of knockdown was selected for subsequent experiments. In selected and mock-transfected clones, the degree of SR knockdown was also evaluated by way of fluorescence-activated cell sorting (FACS) analysis and western blot analysis as described.[26]

The two cell lines—mock-transfected clone (transfected with control vector) and the SR knockdown clone (80% knockdown efficiency of the message by real-time PCR [data not shown] and 50% knockdown of protein expression by FACS)—were then treated with 0.2% BSA (basal) or secretin (100 nM for 5 minutes) before evaluation of cAMP levels by way of RIA[4,7,9,18] or 0.2% BSA (basal) or secretin (100 nM) before measuring proliferation by way of MTS assay (48-hour incubation). The mock-transfected and SR knockdown clones in large cholangiocytes were incubated in culture medium before evaluating basal proliferative activity by MTS proliferation assay (after incubation for 6, 24, 48, and 72 hours).

Statistical Analysis. All data are expressed as the mean ± SEM. Differences between groups were analyzed using the Student unpaired *t* test when two

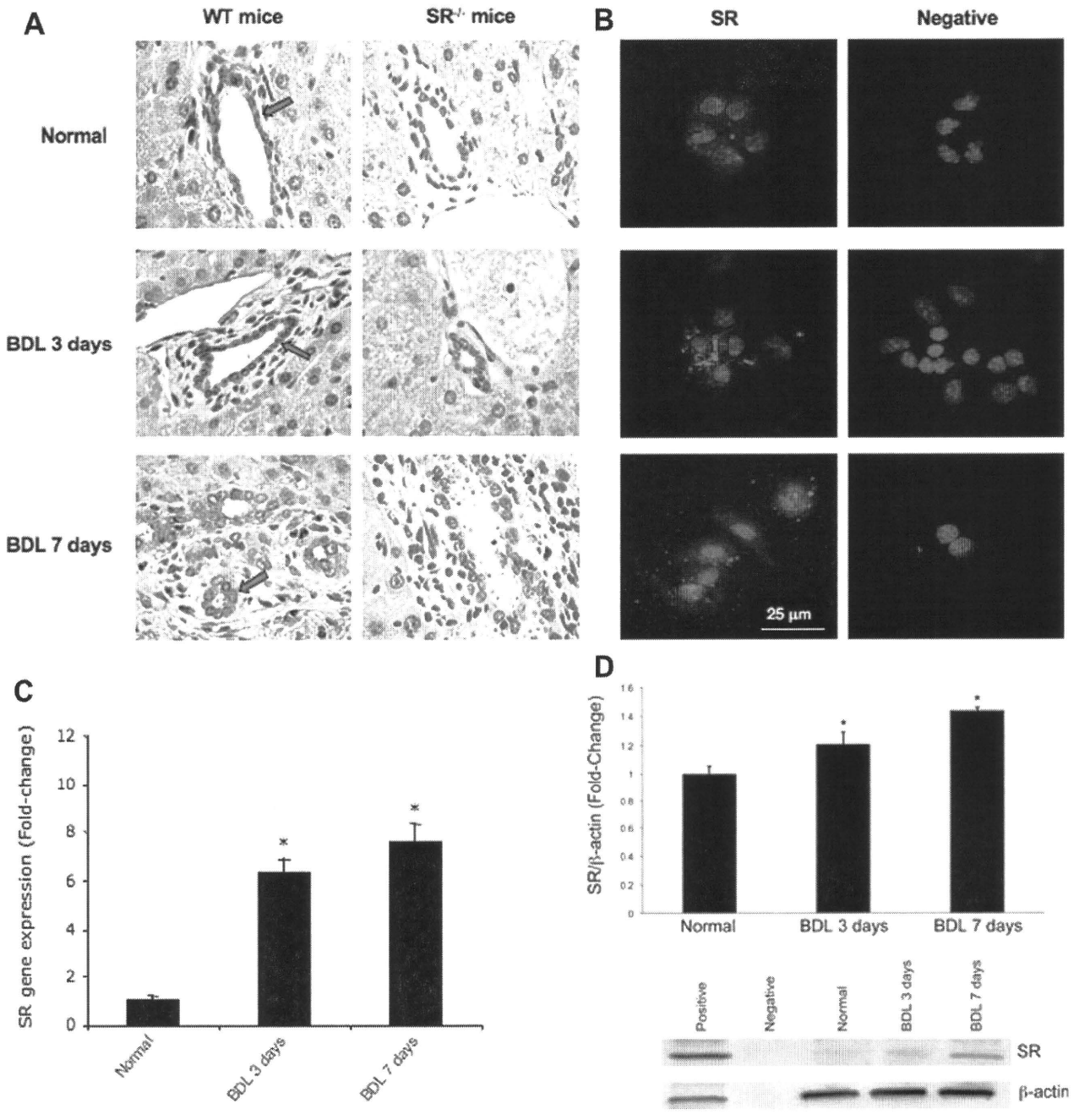

Fig. 1. Evaluation of SR expression by (A) immunohistochemistry in liver sections from WT and $SR^{-/-}$ normal mice, and mice with BDL for 3 and 7 days, (B) immunofluorescence, (C) real-time PCR, and (D) immunoblots in freshly isolated large cholangiocytes from normal and 3- and 7-day BDL WT mice. (A) Large bile ducts from normal and BDL WT mice express SR (red arrows). Original magnification ×40. (B) Specific immunoreactivity for SR in representative fields is shown in red; cell nuclei were stained with 4′,6-diamidino-2-phenylindole (blue). Scale bar = 25 μm. (C,D) Data are expressed as the mean ± SEM of six experiments. *$P < 0.05$ versus normal.

groups were analyzed, and by way of analysis of variance when more than two groups were analyzed, followed by an appropriate *post hoc* test.

Results

Evaluation of Secretin Receptor Expression. In liver sections, we demonstrated that large but not small bile ducts from normal and BDL WT mice express SR (Fig. 1A and Table 1). The expression of SR in large bile ducts was higher in: normal WT mice treated with secretin compared to saline-treated mice (Table 1) and WT BDL compared with normal WT mice (Table 1). There was no positive staining for SR in bile ducts from normal and BDL $SR^{-/-}$ mice (Fig. 1A). The expression of SR was confirmed by way of

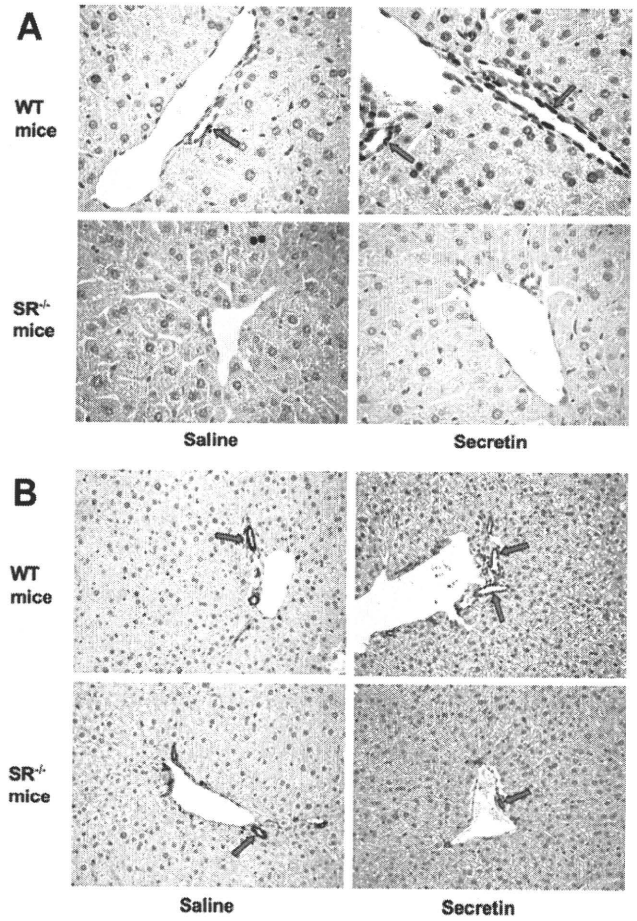

Fig. 2. Evaluation of the number of (A) large PCNA-positive cholangiocytes and (B) large IBDM in normal mice treated with saline or secretin for 1 week. In WT mice treated with secretin, there was an increase in the number of (A) large PCNA-positive cholangiocytes (red arrows) and (B) large IBDM (red arrows) compared with normal WT mice treated with saline. Original magnification ×40 (A) and ×20 (B).

immunofluorescence in large cholangiocytes purified from normal and BDL WT mice (Fig. 1B). Real-time PCR and immunoblot assay revealed that the expression of SR messenger RNA and protein was higher in large BDL cholangiocytes compared with normal large cholangiocytes (Fig. 1C,D).

Evaluation of Liver Weight, Lobular Necrosis, Cholangiocyte Apoptosis, and Proliferation. No significant differences in body weight and mortality rates were observed among the experimental groups of Table 1. No difference in lobular necrosis was observed in normal WT and $SR^{-/-}$ mice, whereas the typical necrosis present in the BDL model showed only a smaller increase (not significant) in $SR^{-/-}$ BDL mice compared with WT BDL mice. The chronic administration of secretin to normal WT mice increased the percentage of large PCNA-positive cholangiocytes and large IBDM compared with normal WT mice treated with saline (Fig. 2A,B and Table 1); secretin did not increase the proliferation of small ducts that do not express SR (not shown).[5] In normal $SR^{-/-}$ mice, secretin did not induce changes in cholangiocyte proliferation or apoptosis (Fig. 2A,B and Table 1). Following BDL, there was an increase in the percentage of PCNA expressing cholangiocytes and IBDM in large bile ducts compared with normal mice (Fig. 3A,B and Table 1). Similar to previous studies,[16] large IBDM was enhanced in parallel with the increased duration of BDL (Fig. 3B and Table 1). Knockout of SR reduces large cholangiocyte proliferation and large IBDM induced by BDL[5,20] compared with WT BDL mice (Fig. 3A,B and Table 1).

Evaluation of Proliferation, cAMP Levels, and Phosphorylation of ERK1/2 in Isolated Large Cholangiocytes. In large cholangiocytes from 7-day $SR^{-/-}$ BDL mice, there was decreased PCNA expression compared with cholangiocytes from WT BDL mice (Fig. 4A). Basal cAMP levels of large cholangiocytes from $SR^{-/-}$ BDL mice were significantly lower than

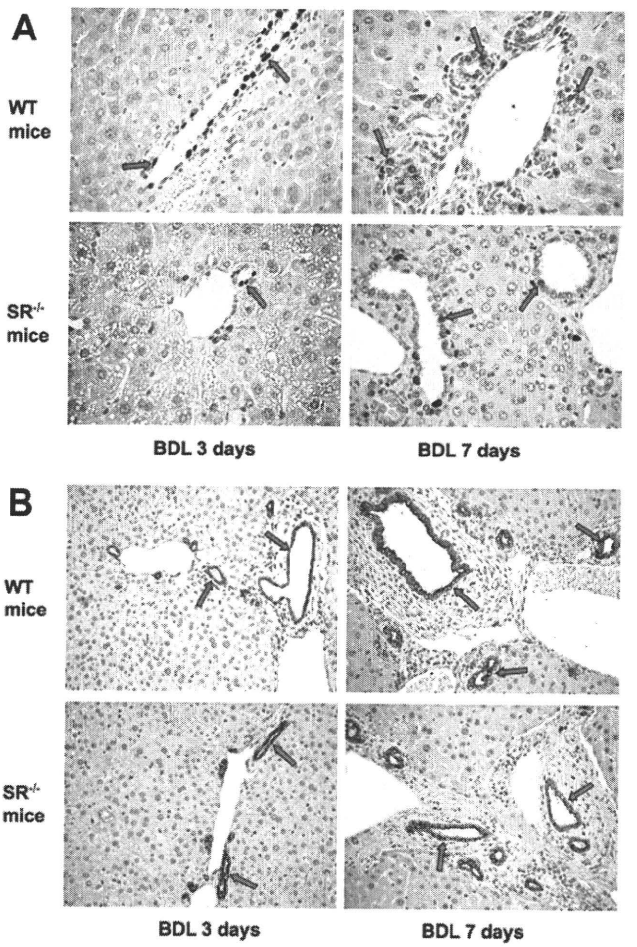

Fig. 3. Evaluation of the number of (A) large PCNA-positive cholangiocytes and (B) large IBDM in WT and $SR^{-/-}$ mice with BDL for 3 and 7 days. Original magnification ×40 (A) and ×20 (B).

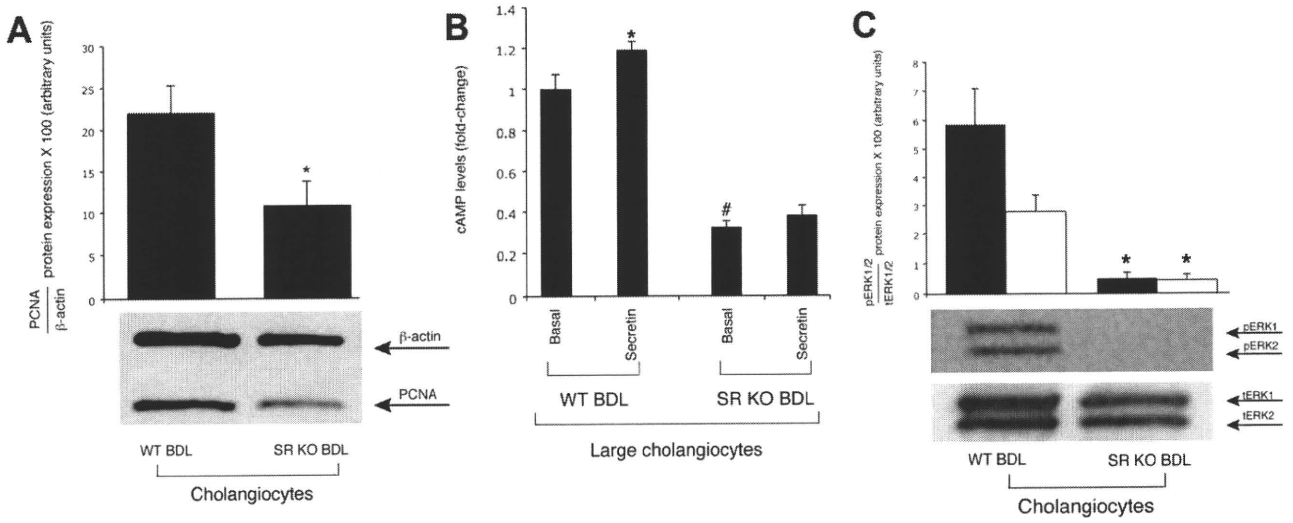

Fig. 4. Evaluation of (A) PCNA protein expression, (B) basal and secretin-stimulated cAMP levels, and (C) ERK1/2 phosphorylation in large cholangiocytes from WT and $SR^{-/-}$ 7-day BDL mice. (A) Data are expressed as the mean ± SEM of seven experiments. *$P < 0.05$ versus PCNA protein of large cholangiocytes from WT 7-day BDL mice. (B) Data are expressed as the mean ± SEM of seven experiments. *$P < 0.05$ versus 0.05 versus basal cAMP levels of large cholangiocytes from WT 7-day BDL mice. (C) Data are expressed as the mean ± SEM of seven experiments. *$P < 0.05$ versus 0.05 versus ERK1/2 phosphorylation of large cholangiocytes from WT 7-day BDL mice.

the corresponding levels of cholangiocytes from WT BDL mice (Fig. 4B). Secretin increased cAMP levels of large cholangiocytes from WT (but not $SR^{-/-}$) BDL mice (Fig. 4B). In large cholangiocytes from $SR^{-/-}$ BDL mice, there was a decreased ERK1/2 phosphorylation compared with large cholangiocytes from WT BDL mice (Fig. 4C).

Secretin Stimulates In Vitro Large Cholangiocyte Proliferation. Large (but not small) cholangiocytes proliferate after the administration of secretin (Fig. 5A). Secretin-stimulation of large cholangiocyte proliferation was blocked by H89 and partially by the MEK inhibitor, PD98059 (Fig. 5A). Secretin increased PCNA expression of large cholangiocytes, an increase that was blocked by H89 and PD98059 (Fig. 5B). There was increased PKA activity (Fig. 5C) and ERK1/2 phosphorylation (Fig. 5D) in large cholangiocytes treated with secretin compared to BSA-treated cells.

Silencing of the Secretin Receptor Gene Decreases the Proliferative Capacity of Large Cholangiocytes. The knockdown of SR protein expression by 50%, as demonstrated by FACS (Fig. 6B), was confirmed by way of western blot analysis (Fig. 6A). When we knocked down the gene for SR in large cholangiocytes, secretin did not increase cAMP levels (Fig. 6C) and proliferation (Fig. 6D, 48 hours of incubation) in these cells compared with the increase shown in large mock-transfected cholangiocytes. In support of the hypothesis that SR is a key trophic regulator in the regulation of biliary growth, there was a decrease in the basal proliferative capacity (Fig. 7) of SR-silenced large cholangiocytes compared with large mock-transfected cholangiocytes.

Discussion

In our study, we show that SR is an important trophic regulator sustaining large cholangiocyte proliferation during extrahepatic cholestasis. In the $SR^{-/-}$ mouse model, we show that proliferation of large cholangiocytes[12,14] is reduced (≈50%) during BDL compared with BDL WT mice, concomitant with elevation of biliary apoptosis. The reduction of cholangiocyte hyperplasia was associated with a decrease in both basal and secretin-stimulated cAMP levels and phosphorylation of ERK1/2 in large cholangiocytes compared with BDL cholangiocytes. *In vitro*, secretin increased the proliferation of large cholangiocytes by activation of cAMP→PKA→ERK1/2 signaling. Silencing of the SR gene induces a decrease in the basal proliferative capacity of large cholangiocytes compared with large mock-transfected cholangiocytes.

In our evaluation of SR expression, we found a time-dependent increase in the expression of SR in large cholangiocytes during BDL compared with normal large cholangiocytes. This finding was consistent with previous studies showing that: (1) in the rodent liver SR is only expressed by large cholangiocytes,[1,4,5,9,12] (2) SR expression is up-regulated following BDL ligation in large cholangiocytes,[14,17] and (3) the extent of secretin effects on cholangiocyte

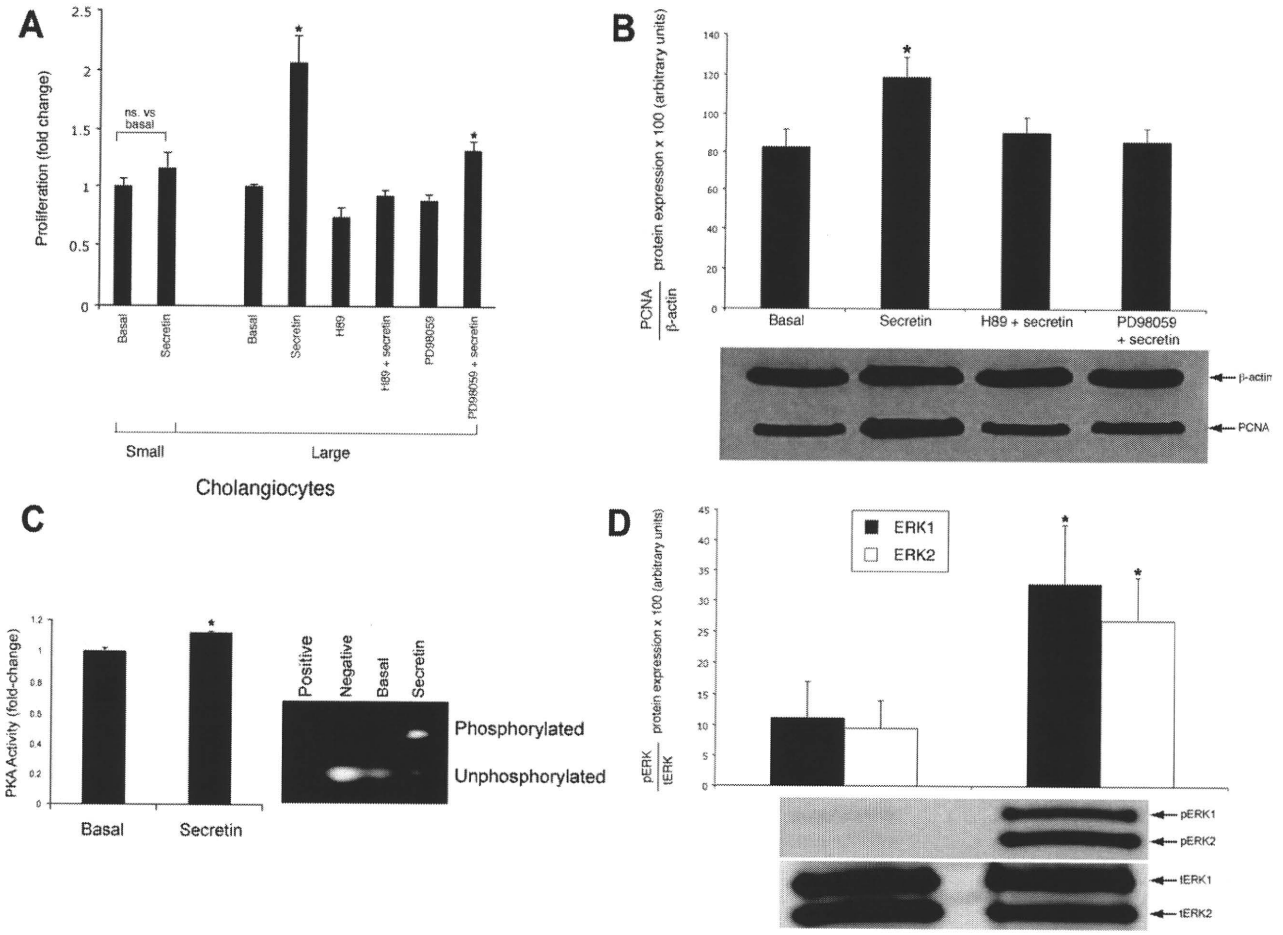

Fig. 5. (A) Effect of 0.2% BSA (basal) or secretin (100 nM) for 48 hours at 37°C on the proliferation of small and large cholangiocytes (MTS assay). Data are expressed as the mean ± SEM of 14 experiments. *$P < 0.05$ versus its corresponding basal value. (B) Data are expressed as the mean ± SEM of 14 experiments. *$P < 0.05$ versus its corresponding basal value. Secretin increased (C) PKA activity (n = 4) and (D) ERK1/2 phosphorylation (n =7) in large cholangiocytes compared with large cholangiocytes treated with BSA. *$P < 0.05$ versus its corresponding basal value.

functions parallel with the duration of BDL.[16] This finding parallels recent findings that mouse cholangiocytes share a similar heterogeneous profile as rat cholangiocytes[5] and freshly isolated and immortalized large mouse cholangiocytes are the only cell types to express the SR.[5,8,14] In human, SR expression is present in the biliary tract in normal bile ducts and ductules and the majority of cholangiocarcinomas, but is not present in hepatocytes or hepatocellular carcinoma.[26,27] Consistent with animal models of cholestasis, SR expression was up-regulated in ductular reactions in liver cirrhosis.[27]

In our *in vivo* model, the level of the reduction of cholangiocyte proliferation is consistent with the paradigm that cholangiocyte proliferation is regulated in autocrine and paracrine mechanisms by a number of stimulatory neurohormonal factors.[18,20,28] In a knockout mouse model for α-calcitonin gene-related peptide, the lack of circulating α-calcitonin gene-related peptide also reduces biliary proliferation during BDL to a similar degree as the lack of SR,[20] which indicates that the regulation of biliary proliferation during extrahepatic cholestasis is multifactorial and a complex regulatory system.[18,20,28]

The trophic effects of secretin were dependent upon the activation of the cAMP/PKA/ERK1/2 signaling. The second messenger system, cAMP, is a key factor for the function of large cholangiocytes.[1,4,7,9,13] Secretin stimulates bicarbonate secretion of large bile ducts through activation of cAMP-dependent CFTR→Cl^-/HCO_3^- anion exchanger 2.[1,4,7,9,13] Also, the activation of the cAMP/PKA/ERK1/2 pathway modulates cholangiocyte proliferation.[12,15,18,29] In fact, the direct stimulation of adenylyl cyclase activity by the chronic administration of forskolin stimulates normal cholangiocyte proliferation both *in vivo* and *in vitro*, which is associated with activation of the PKA/Src/MEK/ERK1/2 pathway.[29] Maintenance of cAMP levels by

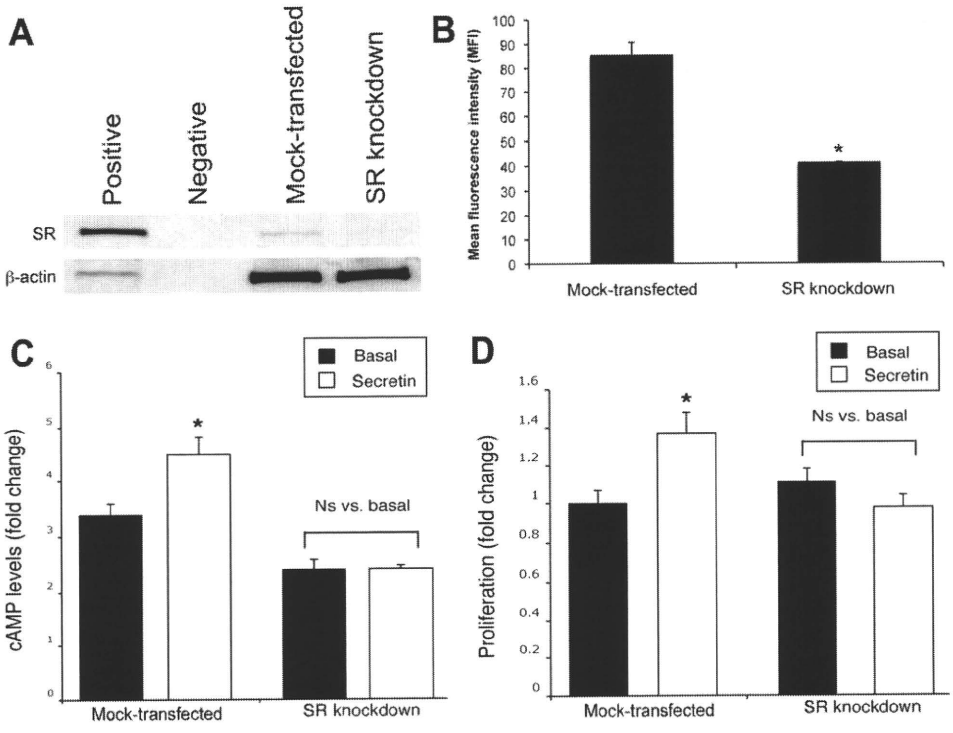

Fig. 6. Knockdown of secretin receptor protein expression in large cholangiocytes was evaluated by (A) western blotting and (B) FACS. Effect secretin receptor gene silencing on the effects of secretion on (C) cAMP levels, and (D) proliferation (by MTS assays) of large cholangiocytes. Data are expressed as the mean ± SEM of six experiments. *$P < 0.05$ versus its corresponding value of mock-transfected large cholangiocytes.

forskolin administration prevents the impairment of cholangiocyte proliferation and enhancement of biliary apoptosis induced by vagotomy.[30] Furthermore, Banales et al. have shown[31] that cAMP stimulates cholangiocyte proliferation through two downstream effectors (i.e., PKA and Epacs) in an animal model of autosomal recessive polycystic kidney disease. Down-regulation of cAMP levels and cAMP-dependent signaling reduces biliary growth and increases cholangiocyte damage by apoptosis.[12,14,20,30] The involvement of the cAMP-dependent ERK1/2 pathway in secretin-dependent biliary proliferation during cholestasis was

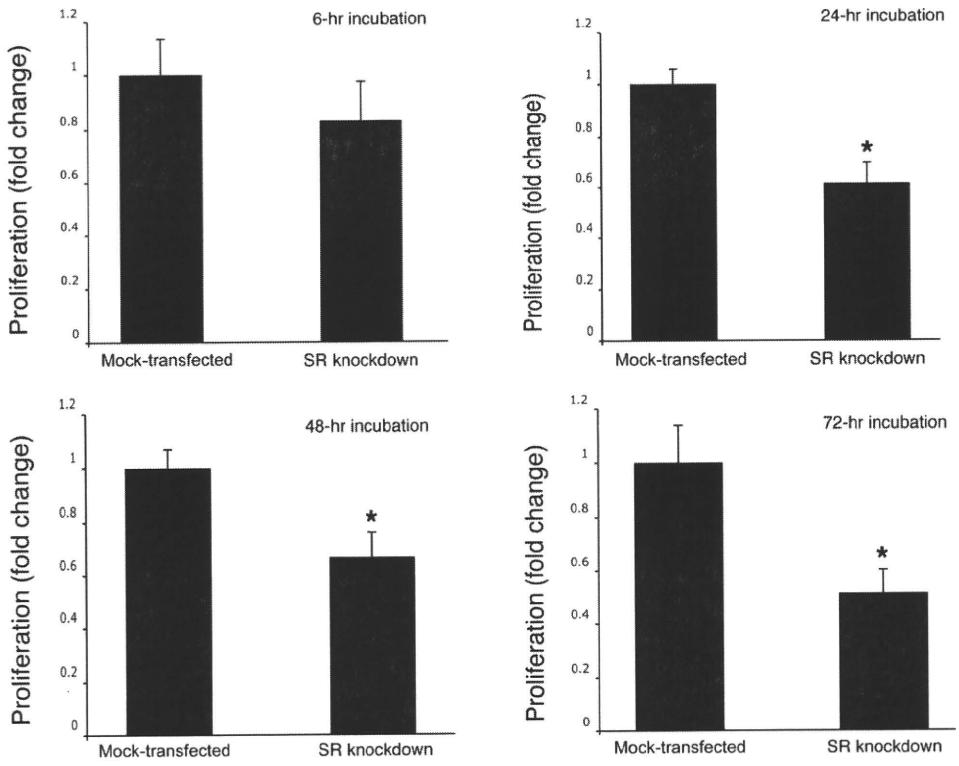

Fig. 7. Effect of secretin receptor gene silencing on the basal proliferative activity of large cholangiocytes following incubation for 6, 24, 48, and 72 hours with 0.2% BSA (MTS assay). Data are expressed as the mean ± SEM of four experiments. *$P < 0.05$ versus its corresponding value of mock-transfected large cholangiocytes.

confirmed in BDL $SR^{-/-}$ mice, which had reduced levels of phosphorylated ERK1/2 in isolated large cholangiocytes. As expected, large cholangiocytes isolated from $SR^{-/-}$ did not respond to secretin, which was evidenced by lack of accumulation of intracellular cAMP levels.

Finally, we demonstrated that SR expression is critical for basal cholangiocyte proliferation in large mouse cholangiocytes that have stable knockdown of SR by transfection with short hairpin RNA for SR. These SR stable knockdown cells displayed decreased basal and secretin-stimulated proliferative capacity compared with control-transfected cholangiocytes. As expected, these stable knockdown SR cells lacked secretin-stimulated intracellular cAMP levels. Decreased basal proliferative rates that we observed in the cells with stable knockdown of SR compared with the mock-transfected controls are suggestive of the regulation of the basal proliferative rates by secretin perhaps in an autocrine mechanism. Consistent with our current study, we have previously shown that secretin stimulates the proliferation of two normal human cholangiocyte cell lines: H-69 and HiBEpiC.[26] Collectively, the findings of our study revealed that secretin is a trophic factor for cholangiocytes that differentially regulated the growth of large cholangiocytes by acting on the specifically expressed SR under normal and pathological conditions.

De novo SR expression in small cholangiocytes is often found in models of liver damage that alter the SR-dependent functional capacity of large cholangiocytes such as CCl_4 acute hepatoxicity.[14] We also have preliminary findings (unpublished data) that suggest that secretin has a protective role versus CCl_4-induced damage of large cholangiocytes.[14] These findings are consistent with the lack of secretin-dependent signaling resulting in an increase in the basal apoptotic activity in cells lacking SR that we observed in the SR knockdown cells. In addition, our other studies in which large cholangiocyte damage was prevented by administration of bile acids (such as taurocholate)[32] and cAMP agonists[30] suggest that secretin, a cAMP agonist, would have a role as a protective factor during large bile duct damage. Further studies are necessary to confirm this role, but are suggestive that secretin or other cAMP agonists could prevent biliary loss in ductopenia pathologies such as drug-induced vanishing bile duct syndrome or graft versus host disease.

The discovery of a novel proproliferative function of secretin in cholangiocytes, along with the demonstration that *in vitro* and *in vivo* molecular manipulations of the SR gene ablated the proliferative and apoptotic responses of large cholangiocytes, may shed light on the development of new therapeutic approach for the management of cholestatic liver diseases. Overexpression of SR or secretin administration might open new avenues for the treatment of ductopenic liver diseases.

References

1. Alpini G, Glaser S, Robertson W, Rodgers RE, Phinizy JL, Lasater J, et al. Large but not small intrahepatic bile ducts are involved in secretin-regulated ductal bile secretion. Am J Physiol Gastrointest Liver Physiol 1997;272:G1064-G1074.
2. Alpini G, Lenzi R, Sarkozi L, Tavoloni N. Biliary physiology in rats with bile ductular cell hyperplasia. Evidence for a secretory function of proliferated bile ductules. J Clin Invest 1988;81:569-578.
3. Kanno N, LeSage G, Glaser S, Alpini G. Regulation of cholangiocyte bicarbonate secretion. Am J Physiol Gastrointest Liver Physiol 2001; 281:G612-G625.
4. Alpini G, Roberts S, Kuntz SM, Ueno Y, Gubba S, Podila PV, et al. Morphological, molecular, and functional heterogeneity of cholangiocytes from normal rat liver. Gastroenterology 1996;110:1636-1643.
5. Glaser S, Gaudio E, Rao A, Pierce LM, Onori P, Franchitto A, et al. Morphological and functional heterogeneity of the mouse intrahepatic biliary epithelium. Lab Invest 2009;89:456-469.
6. Martinez-Anso E, Castillo JE, Diez J, Medina JF, Prieto J. Immunohistochemical detection of chloride/bicarbonate anion exchangers in human liver. HEPATOLOGY 1994;19:1400-1406.
7. Kato A, Gores GJ, LaRusso NF. Secretin stimulates exocytosis in isolated bile duct epithelial cells by a cyclic AMP-mediated mechanism. J Biol Chem 1992;267:15523-15529.
8. Ueno Y, Alpini G, Yahagi K, Kanno N, Moritoki Y, Fukushima K, et al. Evaluation of differential gene expression by microarray analysis in small and large cholangiocytes isolated from normal mice. Liver Int 2003;23:449-459.
9. Alpini G, Ulrich C, Roberts S, Phillips JO, Ueno Y, Podila PV, et al. Molecular and functional heterogeneity of cholangiocytes from rat liver after bile duct ligation. Am J Physiol Gastrointest Liver Physiol 1997; 272:G289-G297.
10. Banales JM, Arenas F, Rodriguez-Ortigosa CM, Saez E, Uriarte I, Doctor RB, et al. Bicarbonate-rich choleresis induced by secretin in normal rat is taurocholate-dependent and involves AE2 anion exchanger. HEPATOLOGY 2006;43:266-275.
11. Lazaridis KN, Strazzabosco M, LaRusso NF. The cholangiopathies: disorders of biliary epithelia. Gastroenterology 2004;127:1565-1577.
12. Alpini G, Glaser S, Ueno Y, Pham L, Podila PV, Caligiuri A, et al. Heterogeneity of the proliferative capacity of rat cholangiocytes after bile duct ligation. Am J Physiol Gastrointest Liver Physiol 1998;274: G767-G775.
13. LeSage G, Glaser S, Gubba S, Robertson WE, Phinizy JL, Lasater J, et al. Regrowth of the rat biliary tree after 70% partial hepatectomy is coupled to increased secretin-induced ductal secretion. Gastroenterology 1996;111:1633-1644.
14. LeSage G, Glaser S, Marucci L, Benedetti A, Phinizy JL, Rodgers R, et al. Acute carbon tetrachloride feeding induces damage of large but not small cholangiocytes from BDL rat liver. Am J Physiol Gastrointest Liver Physiol 1999;276:G1289-G1301.
15. Alvaro D, Onori P, Metalli VD, Svegliati-Baroni G, Folli F, Franchitto A, et al. Intracellular pathways mediating estrogen-induced cholangiocyte proliferation in the rat. HEPATOLOGY 2002;36:297-304.
16. Alpini G, Lenzi R, Zhai WR, Slott PA, Liu MH, Sarkozi L, et al. Bile secretory function of intrahepatic biliary epithelium in the rat. Am J Physiol Gastrointest Liver Physiol 1989;257:G124-G133.
17. Alpini G, Ulrich CD 2nd, Phillips JO, Pham LD, Miller LJ, LaRusso NF. Upregulation of secretin receptor gene expression in rat

cholangiocytes after bile duct ligation. Am J Physiol Gastrointest Liver Physiol 1994;266:G922-G928.
18. Glaser S, Benedetti A, Marucci L, Alvaro D, Baiocchi L, Kanno N, et al. Gastrin inhibits cholangiocyte growth in bile duct-ligated rats by interaction with cholecystokinin-B/Gastrin receptors via D-myo-inositol 1,4,5-triphosphate-, $Ca^{(2+)}$-, and protein kinase C alpha-dependent mechanisms. HEPATOLOGY 2000;32:17-25.
19. Lam IP, Siu FK, Chu JY, Chow BK. Multiple actions of secretin in the human body. Int Rev Cytol 2008;265:159-190.
20. Glaser S, Ueno Y, DeMorrow S, Chiasson VL, Katki KA, Venter J, et al. Knockout of alpha-calcitonin gene-related peptide reduces cholangiocyte proliferation in bile duct ligated mice. Lab Invest 2007;87: 914-926.
21. Chu JY, Chung SC, Lam AK, Tam S, Chung SK, Chow BK. Phenotypes developed in secretin receptor-null mice indicated a role for secretin in regulating renal water reabsorption. Mol Cell Biol 2007;27: 2499-2511.
22. Miyoshi H, Rust C, Roberts PJ, Burgart LJ, Gores GJ. Hepatocyte apoptosis after bile duct ligation in the mouse involves Fas. Gastroenterology 1999;117:669-677.
23. DeMorrow S, Francis H, Gaudio E, Ueno Y, Venter J, Onori P, et al. Anandamide inhibits cholangiocyte hyperplastic proliferation via activation of thioredoxin 1/redox factor 1 and AP-1 activation. Am J Physiol Gastrointest Liver Physiol 2008;294:G506-G519.
24. Strausberg RL, Feingold EA, Grouse LH, Derge JG, Klausner RD, Collins FS, et al. Generation and initial analysis of more than 15,000 full-length human and mouse cDNA sequences. Proc Natl Acad Sci USA 2002;99:16899-16903.
25. Baumgardner JN, Shankar K, Hennings L, Badger TM, Ronis MJ. A new model for nonalcoholic steatohepatitis in the rat utilizing total enteral nutrition to overfeed a high-polyunsaturated fat diet. Am J Physiol Gastrointest Liver Physiol 2008;294:G27-G38.
26. Onori P, Wise C, Gaudio E, Franchitto A, Francis H, Carpino G, et al. Secretin inhibits cholangiocarcinoma growth via dysregulation of the cAMP-dependent signaling mechanisms of secretin receptor. Int J Cancer 2009; doi:10.1002/ijc.25028.
27. Korner M, Hayes GM, Rehmann R, Zimmermann A, Scholz A, Wiedenmann B, et al. Secretin receptors in the human liver: expression in biliary tract and cholangiocarcinoma, but not in hepatocytes or hepatocellular carcinoma. J Hepatol 2006;45:825-835.
28. Alvaro D, Mancino MG, Glaser S, Gaudio E, Marzioni M, Francis H, et al. Proliferating cholangiocytes: a neuroendocrine compartment in the diseased liver. Gastroenterology 2007;132:415-431.
29. Francis H, Glaser S, Ueno Y, LeSage G, Marucci L, Benedetti A, et al. cAMP stimulates the secretory and proliferative capacity of the rat intrahepatic biliary epithelium through changes in the PKA/Src/MEK/ERK1/2 pathway. J Hepatol 2004;41:528-537.
30. LeSage G, Alvaro D, Benedetti A, Glaser S, Marucci L, Baiocchi L, et al. Cholinergic system modulates growth, apoptosis, and secretion of cholangiocytes from bile duct-ligated rats. Gastroenterology 1999;117: 191-199.
31. Banales JM, Masyuk TV, Gradilone SA, Masyuk AI, Medina JF, LaRusso NF. The cAMP effectors Epac and protein kinase a (PKA) are involved in the hepatic cystogenesis of an animal model of autosomal recessive polycystic kidney disease (ARPKD). HEPATOLOGY 2009;49: 160-174.
32. Marzioni M, LeSage GD, Glaser S, Patel T, Marienfeld C, Ueno Y, et al. Taurocholate prevents the loss of intrahepatic bile ducts due to vagotomy in bile duct-ligated rats. Am J Physiol Gastrointest Liver Physiol 2003;284:G837-G852.

Adenosine Triphosphate Release and Purinergic (P2) Receptor–Mediated Secretion in Small and Large Mouse Cholangiocytes

Kangmee Woo,[1] Meghana Sathe,[1] Charles Kresge,[1] Victoria Esser,[2] Yoshiyuki Ueno,[5] Julie Venter,[3] Shannon S. Glaser,[3] Gianfranco Alpini,[3,4] and Andrew P. Feranchak[1]

Adenosine triphosphate (ATP) is released from cholangiocytes into bile and is a potent secretogogue by increasing intracellular Ca^{2+} and stimulating fluid and electrolyte secretion via binding purinergic (P2) receptors on the apical membrane. Although morphological differences exist between small and large cholangiocytes (lining small and large bile ducts, respectively), the role of P2 signaling has not been previously evaluated along the intrahepatic biliary epithelium. The aim of these studies therefore was to characterize ATP release and P2-signaling pathways in small (MSC) and large (MLC) mouse cholangiocytes. The findings reveal that both MSCs and MLCs express P2 receptors, including P2X4 and P2Y2. Exposure to extracellular nucleotides (ATP, uridine triphosphate, or 2′,3′-O-[4-benzoyl-benzoyl]-ATP) caused a rapid increase in intracellular Ca^{2+} concentration and in transepithelial secretion (I_{sc}) in both cell types, which was inhibited by the Cl^- channel blockers 5-nitro-2-(-3-phenylpropylamino)-benzoic acid (NPPB) or niflumic acid. In response to mechanical stimulation (flow/shear or cell swelling secondary to hypotonic exposure), both MSCs and MLCs exhibited a significant increase in the rate of exocytosis, which was paralleled by an increase in ATP release. Mechanosensitive ATP release was two-fold greater in MSCs compared to MLCs. ATP release was significantly inhibited by disruption of vesicular trafficking by monensin in both cell types. *Conclusion*: These findings suggest the existence of a P2 signaling axis along intrahepatic biliary ducts with the "upstream" MSCs releasing ATP, which can serve as a paracrine signaling molecule to "downstream" MLCs stimulating Ca^{2+}-dependent secretion. Additionally, in MSCs, which do not express the cystic fibrosis transmembrane conductance regulator, Ca^{2+}-activated Cl^- efflux in response to extracellular nucleotides represents the first secretory pathway clearly identified in these cholangiocytes derived from the small intrahepatic ducts. (HEPATOLOGY 2010;52:1819-1828)

Cholangiocytes, the epithelial cells that form the intrahepatic bile ducts, represent an important component of the bile secretory unit. Although bile formation is initiated at the hepatocyte canalicular membrane, cholangiocytes subsequently modify the composition of bile through regulated ion secretion throughout the network of bile ducts.[1] Interestingly, secretory mechanisms along the intrahepatic bile ducts are not uniform. In all biliary models studied, including human, rat, and mouse bile ducts, cholangiocytes are known to be morphologically and functionally heterogeneous. Large cholangiocytes, from large ducts, express secretin receptors on the basolateral membrane and express cystic fibrosis transmembrane

Abbreviations: AE2, anion exchanger 2; ATP, adenosine triphosphate; Bz-ATP, 2′,3′-O-(4-benzoyl-benzoyl)-ATP; cAMP, cyclic adenosine monophosphate; CFTR, cystic fibrosis transmembrane conductance regulator; fura-2-AM, fura-2-acetoxymethyl ester; IP3, inositol 1,4,5-triphosphate; Isc, transepithelial short-circuit current response; MLC, mouse large cholangiocyte; MSC, mouse small cholangiocyte; NPPB, 5-nitro-2-(-3-phenylpropylamino)-benzoic acid; RT-PCR, reverse transcription polymerase chain reaction; UTP, uridine triphosphate.

From the [1]Department of Pediatrics, and [2]Internal Medicine, University of Texas Southwestern Medical Center, Dallas, TX; [3]Research, Central Texas Veterans Health Care System, Scott & White Digestive Disease Research Center, Scott & White Healthcare, Temple, TX; [4]Department of Medicine, Division Gastroenterology, Texas A&M Health Science Center College of Medicine, Temple, TX; and [5]Tohoku University, School of Medicine, Sendai, Japan.

Received September 21, 2009; accepted July 22, 2010.

This study was supported by the Cystic Fibrosis Foundation (FERANC08G0), the Children's Medical Center Foundation, and the National Institute of Diabetes, Digestive and Kidney Diseases (NIDDK) of the National Institutes of Health, grants DK078587 (to A.P.F.) and DK054811 (to G.A.), and a VA Merit Award (to G.A.).

conductance regulator (CFTR) and the HCO_3^-/Cl^- anion exchanger 2 (AE2) on the apical membrane,[2-4] and hence respond to secretin with an increase in [cAMP] (intracellular cyclic adenosine monophosphate concentration), and subsequent Cl^- and HCO_3^- efflux into the lumen. Conversely, small cholangiocytes, from small ducts, do not express secretin receptors, CFTR, or HCO_3^-/Cl^- exchanger and do not exhibit a secretory response to secretin.[3] In human liver, parallel to the findings observed in the rat and mouse, secretin-stimulated duct secretory activity is heterogeneous, because only medium and large interlobular bile ducts express the Cl^-/HCO_3^- exchanger AE2.[5]

Recently, secretion mediated by extracellular nucleotides (e.g., adenosine triphosphate [ATP]) acting on purinergic (P2) receptors on the luminal membrane of biliary epithelial cells has emerged as functionally important. ATP is present in bile,[6] and binding of ATP to P2 receptors increases K^+,[7,8] and Cl^- efflux from isolated cholangiocytes[9,10] and dramatically increases transepithelial secretion in biliary epithelial monolayers.[10,11] Indeed, the magnitude of the secretory response to ATP is two-fold to three-fold greater than that to cAMP.[10] Interestingly, recent evidence suggests that even cAMP-stimulated bile flow is mediated by ATP release into the duct lumen and stimulation of apical P2 receptors.[12] Together, these studies challenge and extend the conventional model that centers on the concept that cAMP-dependent opening of CFTR-related Cl^- channels is the driving force for cholangiocyte secretion. Rather, the operative regulatory pathways appear to take place within the lumen of intrahepatic ducts, where release of ATP into bile is a final common pathway controlling ductular bile formation. In light of recent studies demonstrating that the mechanical effects of fluid-flow or shear stress at the apical membrane of biliary epithelial cells is a robust stimulus for ATP release,[13] a model emerges in which mechanosensitive ATP release and Cl^- secretion is a dominant pathway regulating biliary secretion.

Although cholangiocytes express a repertoire of both P2X and P2Y receptors,[11,14,15] it is unknown if expression differs between small and large cholangiocytes and/or if functional differences exist in ATP release and signaling along the bile duct. The aim of the current studies therefore was to determine if a potential P2 signaling axis may exist along the bile duct by evaluating mechanosensitive ATP release and exocytosis, P2 receptor expression and function, and secretion mediated by extracellular nucleotides in both small (MSC) and large (MLC) mouse cholangiocytes.

Materials and Methods

Cell Models. Studies were performed in mouse cholangiocytes isolated from normal mice (BALB/c) and immortalized by transfection with the simian virus 40 large-T antigen gene.[4] These cells demonstrate identical properties to freshly isolated small and large mouse cholangiocytes.[3] Cells were maintained in culture as described.[3,4] Additional studies of P2 receptor expression were performed in primary cholangiocytes isolated from C57BL/6 mice (Charles River, Wilmington, MA) as previously described.[16,17] All animal experiments were performed in accordance with a protocol approved by the Scott & White Institutional Animal Care and Use Committee and in accordance with the Guide for the Care and Use of Laboratory Animals published by the U.S. National Institutes of Health (NIH Publication No. 85-23, revised 1996).

Total RNA Isolation and RT-PCR Analysis. Total RNA was extracted using TRIZOL Reagent (Invitrogen, Carlsbad, CA) and 1 μg RNA was reverse transcribed in the presence of 100 pmol oligo-deoxythymidine primer. For reverse transcription polymerase chain reaction (RT-PCR), aliquots of 5% of the total complementary DNA were amplified with TaqDNA polymerase in a reaction mixture containing 20 pmol of 5′ and 3′ primers specifically designed for various P2X and P2Y receptors (Supporting Information Methods and Supporting Information Table 1).

Measurement of Intracellular Ca^{2+} Concentration. MLCs and MSCs were grown to confluence on coverglass (Fig. 2), loaded with 2.5 μg/mL of fura-2-acetoxymethyl ester (fura-2-AM; TEF Laboratories, Austin, TX), placed in a perfusion chamber (RC-25F/PHA; Warner Instruments) on the stage of an inverted fluorescence microscope (Nikon TE2000), and the inflow and outflow ports were connected to a syringe pump. Changes of $[Ca^{2+}]_i$ (the intracellular calcium

Address reprint requests to: Andrew P. Feranchak, M.D., UT Southwestern Medical Center, 5323 Harry Hines Boulevard, Dallas, TX 75390-9063. E-mail: drew.feranchak@UTSouthwestern.edu; fax: 214-648-2673.

View this article online at wileyonlinelibrary.com.
DOI 10.1002/hep.23883
Potential conflict of interest: Nothing to report.
Additional Supporting Information may be found in the online version of this article.

concentration) were measured at excitation wavelength of 340 nm (calcium-bound fura-2-AM) and 380 nm (calcium-free fura-2-AM), and emission wavelength of 510 nm and $[Ca^{2+}]_i$ was calculated.

Immunostaining. Confluent MSCs and MLCs were incubated with acetylated α-tubulin antibody (Sigma), as a marker for the primary cilium, and rhodamine phalloidin (Invitrogen) to label actin. Imaging was performed using a PerkinElmer UltraVIEW ERS spinning disk confocal microscope (PerkinElmer, Boston, MA). Imaris 5.0 (Bitplane, Inc., Saint Paul, MN) was used for three-dimensional volume rendering of z-stacks.

Measurement of Exocytosis. Exocytosis was assessed by real time imaging using the fluorescent dye FM1-43 (Molecular Probes, Inc., Eugene, OR) as previously described.[18] FM1-43 is weakly fluorescent in aqueous solution, but its fluorescence increases >300-fold when it binds plasma membrane and, therefore, it is a useful dye for the measurement of increased plasma membrane due to fusion of vesicle membrane with the plasma membrane during exocytosis.

Measurement of ATP Release. Bulk ATP release was studied from confluent cells using the luciferin-luciferase (L-L) assay as previously described.[13,19,20] Cell swelling was induced by adding water to dilute media 33% and defined shear stress was applied to confluent cells in a parallel plate chamber. All luminescence values are reported as relative change from basal luminescence per total protein level in the sample (measured in micrograms per milliliter) to control for any potential differences in luciferase activity or confluency between samples, respectively. Detailed protocols for measurements of ATP release, ATP degradation, protein levels, and lactate dehydrogenase are described in Supporting Information Methods.

Transepithelial Cl− Secretion. MLCs and MSCs were grown on collagen-coated polycarbonate filters with a pore size of 0.4 μm (Costar, Cambridge, MA) and the transmembrane resistance was measured daily (Evohm voltmeter; World Precision Instruments, Sarasota, FL).[21] Filters were mounted in an Ussing chamber, filled with standard buffer solution, and transepithelial short-circuit current response (I_{sc}) was measured under 0 mV voltage-clamp conditions through agar bridges connected to Ag-AgCl electrodes using an epithelial voltage clamp amplifier (model EC-825; Warner Instruments, MRA International, Naples, FL). The I_{sc} represents the net sum of the transepithelial fluxes of anion and cation and the level of ion secretion.[11] Studies included paired, same-day monolayers to minimize any potential effects of day-to-day variability.

Reagents and Statistics. Detailed descriptions of the reagents, buffer solutions, experimental protocols, and statistical analysis are provided in Supporting Information Materials.

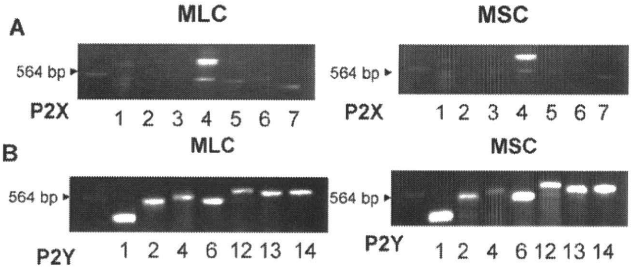

Fig. 1. Mouse cholangiocytes express P2 receptors. Molecular expression of P2X and P2Y receptor subtypes was evaluated by RT-PCR with specific oligonucleotides. (A) P2X receptor expression. P2X4 is the predominant P2X receptor in both mouse large (MLC), left panel, and mouse small (MSC), right panel, cholangiocytes. (B) P2Y receptor expression. Both MLCs and MSCs express multiple P2Y receptor subtypes, including P2Y1, P2Y2, P2Y4, P2Y6, P2Y12, P2Y13, and P2Y14. The arrowhead indicates a 564-base pair (bp) λDNA-Hind III fragment.

Results

Large and Small Cholangiocytes Express a Repertoire of P2X and P2Y Receptors. In both MLCs and MSCs, complementary DNAs were probed with oligonucleotide primers specific to the seven P2X subtypes and seven P2Y subtypes in mouse (shown in Supporting Information Table 1) and amplified using RT-PCR. Representative studies are shown in MLCs and MSCs (Fig. 1), and in primary isolated cholangiocytes (Supporting Information Fig. 1). In both MLCs and MSCs, clear bands corresponding to P2X4 and all seven P2Y receptors (P2Y1, P2Y2, P2Y4, P2Y6, P2Y11, P2Y12, and P2Y13) are present. These results are consistent with previous studies of human and rat biliary cells where a predominance of P2X4 and multiple P2Y receptors were observed.[11,14,15]

Agonist Profile of Nucleotide-Stimulated Ca^{2+} Fluorescence. To establish the functional significance of mouse cholangiocyte P2 receptor expression, MSCs and MLCs were grown to confluence (Fig. 2) and changes in Ca^{2+} fluorescence measured in response to P2Y and P2X agonists. Exposure to ATP, UTP, a P2Y-preferring agonist, or Bz-ATP, a P2X-preferring agonist, all resulted in significant increases in $[Ca^{2+}]_i$ in both MLCs and MSCs (Fig. 3). The ATP-stimulated increase in $[Ca^{2+}]_i$ was abolished by the P2Y receptor blocker, suramin (Fig. 3D). Together, these results demonstrate that P2X4 and P2Y receptors expressed by both MLCs and MSCs are functionally active. No differences were observed between MLCs and MSCs in either the magnitude or kinetics of the Ca^{2+} response to any of the nucleotides.

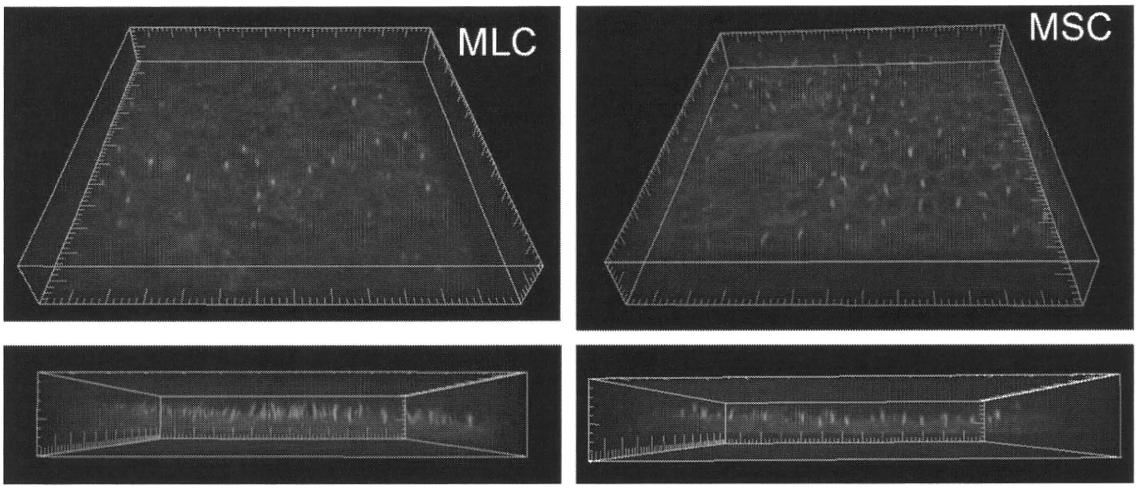

Fig. 2. MLCs and MSCs form polarized monolayers. MLCs (left) and MSCs (right) were cultured on coverglass for 5 days and stained for acetylated α-tubulin, as a cilia marker protein (green), and phalloidin, for actin localization (red). Bottom panels represent *z* axis to highlight cilia. Scale, small hatch marks = 5 μm.

Functional Role for P2 Receptors in Transepithelial Secretion. When cultured as described, both MSCs and MLCs developed an increase in transmembrane resistance by day 3 signifying the development of confluent monolayers with tight junctions (Fig. 4A). When mounted in an Ussing chamber, confluent MLCs and MSCs monolayers exhibited a basal I_{sc}, reflecting transepithelial secretion, which increased dramatically in response to the addition of ATP (100 μM) to the apical chamber (Fig. 4B,C). The nucleotide-stimulated I_{sc} was significantly inhibited by the nonspecific Cl^- channel blocker, 5-nitro-2-(-3-phenylpropylamino)-benzoic acid (NPPB), or by the Ca^{2+}-activated Cl^- channel blocker niflumic acid (Fig. 4C,F). Additionally, preincubation with the IP3 receptor blocker, 2-APB, significantly inhibited the ATP-stimulated increase in I_{sc} in both MLC and MSC (Fig. 4C). In separate experiments, the effect of apical versus basolateral P2 receptor stimulation on the I_{sc} was determined. For both MSCs and MLCs, an increase in the I_{sc} was observed when nucleotides were added to either chamber, consistent with functional expression of P2 receptors on both apical and basolateral membranes. The magnitude of the change in I_{sc} was similar

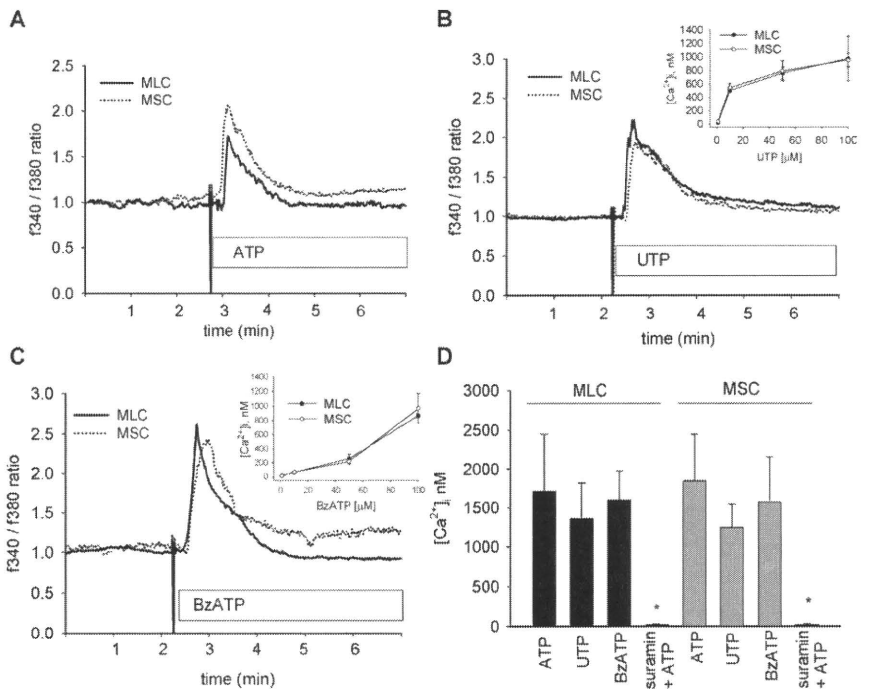

Fig. 3. P2 receptor agonists increase intracellular Ca^{2+} in mouse cholangiocytes. MLCs and MSCs were loaded with fura-2-AM and exposed to extracellular nucleotides, ATP (100 μM), UTP (100 μM), or Bz-ATP (100 μM) as indicated. The *y* axis values represent the ratio of fluorescence at 340 (f340) and at 380 nm (f380). (A-C) Representative studies. The Ca^{2+} fluorescence increased rapidly in both MLCs (solid line) and MSCs (dotted line) upon exposure to nucleotides. Insets in (B) and (C) demonstrate dose-response for respective agonist. (D) Cumulative data. Values represent the maximal $[Ca^{2+}]_i$ in nM. $[Ca^{2+}]_i$ was calculated based on maximal and minimal Ca^{2+} fluorescence obtained by exposure to ionomycin (5 μM) and EGTA (10 mM), respectively (N = 3-6 each). *Suramin significantly inhibits ATP-stimulated [Ca2+]$_i$, $P < 0.05$.

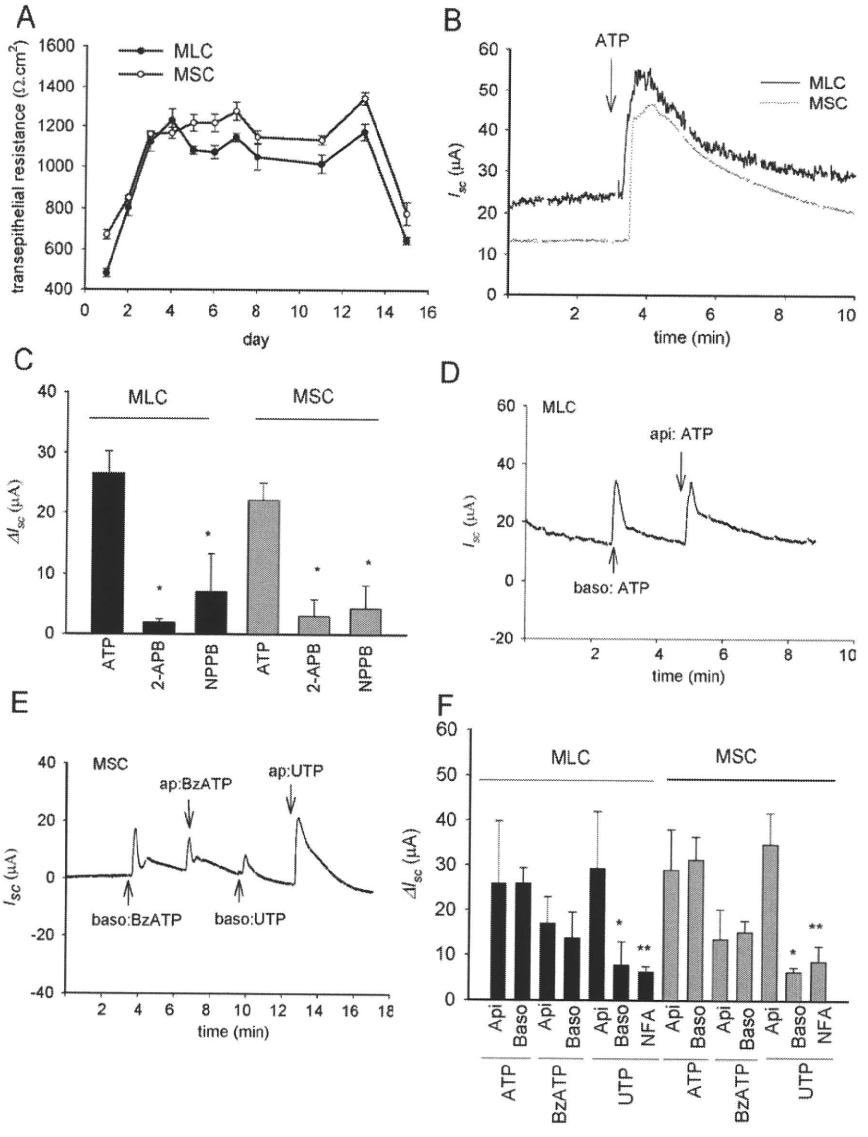

Fig. 4. Mouse cholangiocytes form polarized monolayers and exhibit increases in transepithelial Cl^- secretion in response to extracellular nucleotides. (A) Transmembrane resistance ($\Omega.cm^2$) was measured at the time points indicated in MLCs and MSCs grown on semipermeable filters. (B) Representative tracings of MLCs or MSCs mounted in an Ussing chamber. The *y* axis represents short-circuit current (I_{sc}) across monolayers measured under voltage-clamp conditions (μA). ATP (100 μM), added to the apical chamber, significantly increased I_{sc}. (C) Cumulative data demonstrating effect of 2-APB or NPPB on ATP-stimulated I_{sc}. The *y* axis values are reported as ΔI_{sc} (maximum I_{sc} – basal I_{sc}). *The 2-APB or NPPB significantly inhibit ATP-stimulated ΔI_{sc} ($P < 0.05$, n= 3-9 each). (D) Representative recording of apical or basolateral additions of ATP (100 μM)-stimulated I_{sc} in MLCs. (E) Representative recording of apical or basolateral additions of BzATP (100 μM) and UTP (100 μM) in MSCs. (F) Cumulative data. Values (mean ± standard error of the mean [SEM]) represent Δ I_{sc}. Apical addition (Api) and basolateral addition (Baso), of respective reagent (n = 4-12 each). *Apical addition of UTP increases I_{sc} > than basolateral addition ($P < 0.05$). **Niflumic acid (NFA, 250 μM) inhibits UTP-stimulated I_{sc} ($P < 0.05$).

when nucleotides were added to either apical or basolateral compartments for all nucleotides tested except for UTP which caused a significantly greater increase in I_{sc} when added apically versus basolateral addition. Thus, both MSCs and MLCs express functional P2 receptors on both apical and basolateral membranes. Nucleotide binding to P2 receptors causes an increase in $[Ca^{2+}]_i$, predominantly through an IP3 receptor-dependent mechanism, which stimulates Ca^{2+}-activated Cl^- channels, and results in transepithelial secretion. To our knowledge, these represent the first integrated I_{sc} measurements of transepithelial secretion in mouse cholangiocytes. Furthermore, in MSC, which do not express CFTR, Ca^{2+}-activated Cl^- efflux in response to extracellular nucleotides represents the first secretory pathway clearly identified in these cells derived from the small intrahepatic ducts.

Mechanosensitive ATP Release. In human biliary cells and normal rat cholangiocyte monolayers, mechanical stimulation,[22] shear stress,[13] and cell swelling secondary to hypotonic exposure,[22] have all been identified as significant stimuli for ATP release. Studies were performed to determine if these mechanical stimuli result in a similar increase in the magnitude of ATP release in mouse cholangiocytes. First, in response to hypotonic exposure (33% dilution) to stimulate cell swelling, a rapid and large increase in ATP release was observed in both MLCs and MSCs (Fig. 5A). The magnitude of the response, which peaked within 30 seconds, was significantly greater in MSCs versus MLCs (Fig. 5A,C). Separate studies were performed to assess the effects of shear on ATP release. Under low shear conditions (shear 0.08 dyne/cm^2) no increase in ATP release was observed; however, increasing shear to

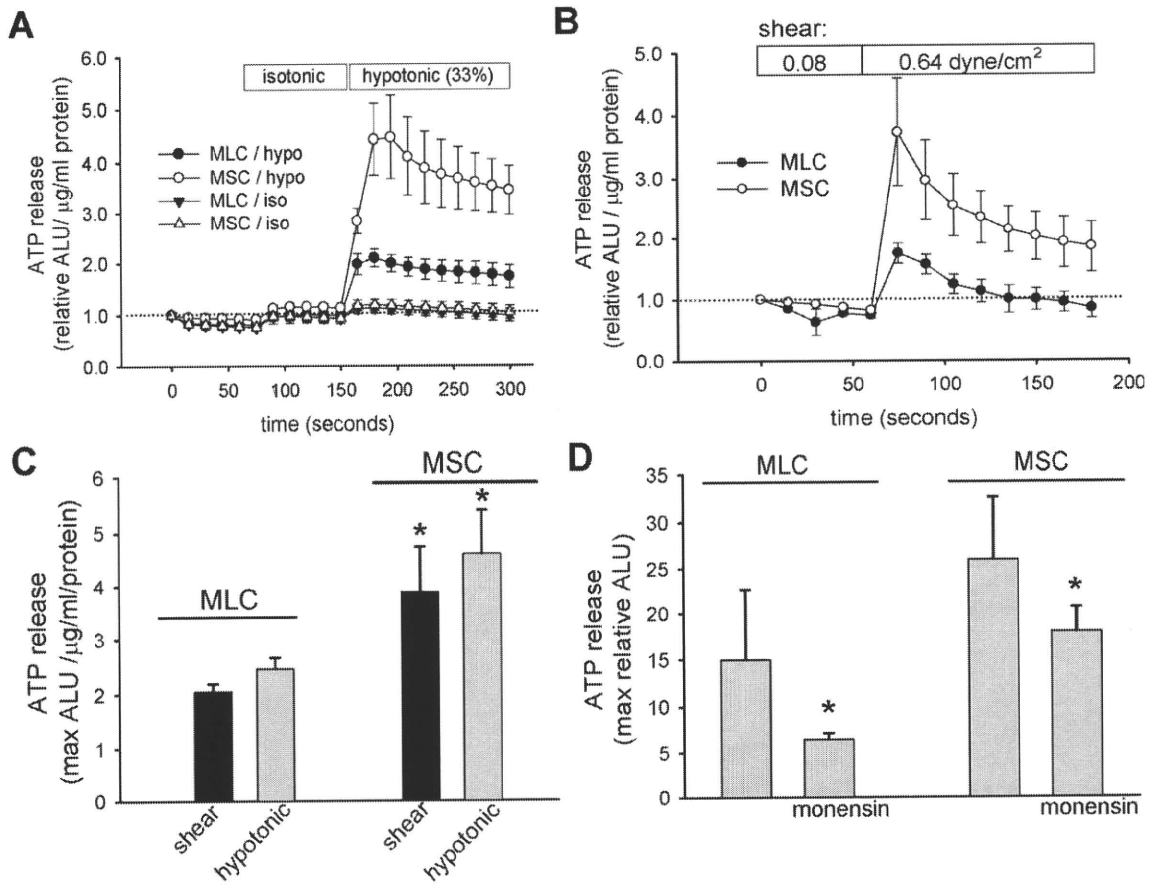

Fig. 5. Mechanosensitive ATP release from mouse cholangiocytes. ATP in the extracellular media was detected using the luciferin-luciferase assay and quantified as arbitrary light units (ALU). The *y* axis represents relative increase from basal luminescence (expressed as relative ALU/ µg/mL protein). (A) Cell swelling-induced ATP release from confluent MLCs and MSCs. Addition of isotonic media to cells led to a small increase in luminescence. Dilution of media 33% by the addition of water (indicated by bar) led to an increase in ATP release in both MSCs (open circles) and MLCs (closed circles) much greater than control cells exposed to only a second isotonic exposure. (B) Shear-stimulated ATP release from confluent MLCs (closed circles) and MSCs (open circles) cells. Cells were perfused with Optimem and 60 µL aliquots were taken from the efflux every 30 seconds, added to standard L-L reagent, and immediately placed in the Luminometer for luminescence measurement. Bars along top indicate length of low flow (shear 0.08 dyne/cm^2) and high flow (shear 0.64 dyne/cm^2) exposure. (C) Cumulative data demonstrating relative ATP release from both MLCs and MSCs in response to shear (0.64 dyne/cm^2, black bar) and hypotonic exposure (33% dilution, gray bar). Values represent maximum ATP concentration within 30 seconds of shear or hypotonic exposure, mean ± SEM. *ATP release is significantly greater in MSCs versus MLCs, $P < 0.05$. (D) Inhibition of vesicular trafficking inhibits swelling-induced ATP release in MLCs and MSCs. *Monensin (100 µM × 30 minutes) significantly inhibits ATP release in response to hypotonic exposure (33% dilution); $P < 0.05$, n = 4-6 each.

0.64 dyne/cm^2 caused a rapid relative increase in ATP release in both MLCs and MSCs, and again the magnitude of the peak response was significantly greater in MSCs versus MLCs ($P < 0.05$, Fig. 5B,C). No difference was noted in lactate dehydrogenase measurements before or after stimulus, for either hypotonic or shear exposure, excluding cell lysis as contributing to measured ATP (data not shown). In other biliary models, ATP release has been linked to exocytosis.[18] To determine if exocytosis contributes to ATP release in MLCs and MSCs, studies were performed in the presence or absence of monensin, a carboxylic ionophore known to dissipate the transmembrane pH gradients in Golgi and lysosomal compartments and disrupt vesicular trafficking. In both MLCs and MSCs, monensin significantly inhibited swelling-induced (33% hypotonic exposure) ATP release (Fig. 5D). Thus, both MSCs and MLCs exhibit mechanosensitive ATP release which is dependent on intact vesicular trafficking pathways. Additionally, the magnitude of mechanosensitive ATP release is significantly greater (~two-fold) in MSCs compared to MLCs.

Mechanosensitive Exocytosis. To determine if the difference in ATP release observed between MSCs and MLCs are the result of generalized differences in total cellular exocytosis, rates of exocytosis were measured in response to mechanical stimuli in both cell types. After equilibration with FM1-43, cells were exposed to hypotonic buffer (33%) which was associated with a rapid increase in fluorescence, reflecting an increase in

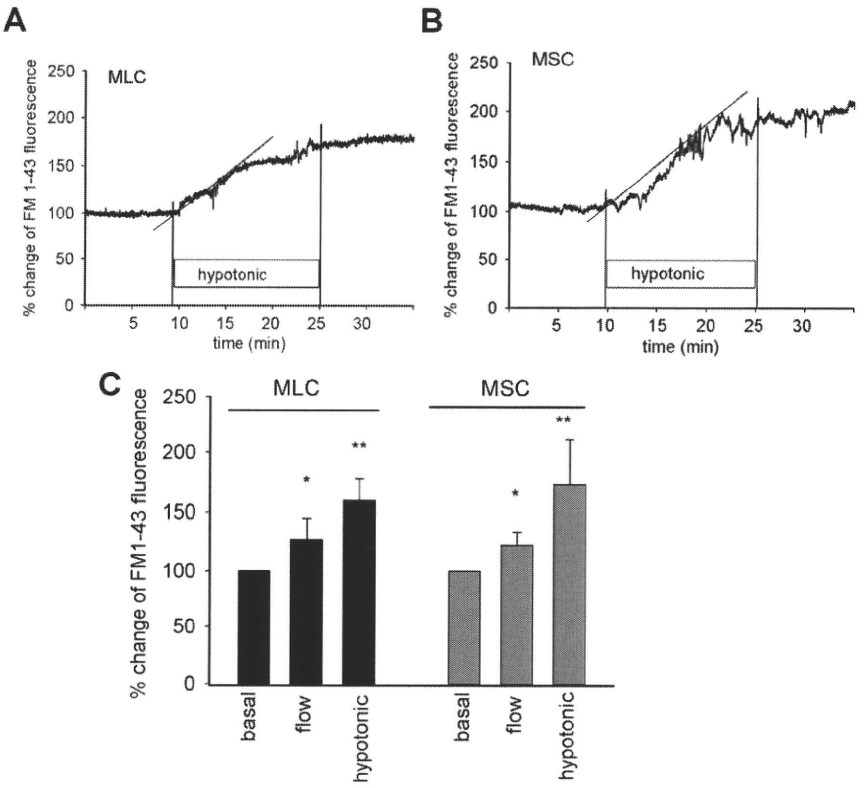

Fig. 6. Mechanosensitive exocytosis. MLCs and MSCs on coverglass were loaded with FM1-43 and exposed to shear or hypotonicity as indicated. The values of the *y* axis represent percent increase in membrane fluorescence. (A,B) Representative figures of swelling-induced exocytosis. FM1-43 fluorescence was stabilized in isotonic buffer before the cells were exposed to hypotonic buffer (33%). Hypotonic exposure rapidly increased plasma membrane fluorescence as a result of vesicular exocytosis in both (A) MLCs and (B) MSCs. Dotted line represents best-fit regression analysis. (E) Cumulative data demonstrating maximum magnitude of exocytosis in both MLCs and MSCs in response to shear (0.64 dyne/cm^2) or hypotonic (33%) exposure. Values represent maximum percent change in FM1-43 fluorescence (n = 5-6 each). *$P < 0.05$ shear versus basal; **$P < 0.05$ hypotonic exposure versus isotonic.

exocytosis (Fig. 6). In separate studies, exposure to shear (0.64 dyne/cm^2) also resulted in an increase in exocytosis (Fig. 6). These findings suggest a functional link between exocytosis and ATP release in both MLCs and MSCs. There was no significant difference noted in the rate or magnitude of exocytosis between MLCs and MSCs in response to either of these mechanical stimuli.

ATP Degradation. The concentration of extracellular ATP in bile is regulated not only through the rate of ATP release, but also through degradation pathways.[23] To determine if differences exist in the kinetics of ATP degradation between MSCs and MLCs, the media bathing confluent cells was loaded with exogenous ATP (10 nM). Changes in bioluminescence were monitored continuously until relative ALU returned to basal levels. As shown in Fig. 7, addition of ATP (10 nM) to MLCs increased relative bioluminescence 2.7-fold. The time course of degradation was described by a single exponential ($y = ae^{-0.038\ min}$, r = 0.99). By comparison, addition of ATP to MSCs increased bioluminescence 2.5-fold with a similar rate of degradation

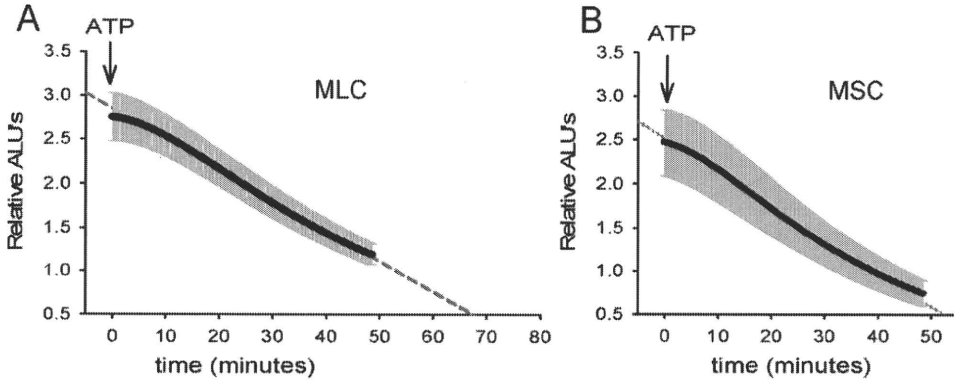

Fig. 7. Kinetics of ATP degradation in mouse cholangiocytes. ATP degradation was assessed after addition of ATP (10 nM, at arrow) to apical membrane of confluent (A) MLCs and (B) MSCs. The *y* axis represents relative arbitrary light units (ALU). Values represent means (black points) ± SEM (gray bars); n = 4 monolayers/time point. Dashed line represents best-fit regression.

described by a single exponential ($y = ae^{-0034\ min}$, r = 0.99). Thus, MLCs and MSCs display functionally similar ATP degradation pathways.

Discussion

The present studies extend the observations regarding the specialized function of cholangiocytes by identifying and characterizing the elements of the purinergic signaling axis in cholangiocytes derived from distinct functional areas along the intrahepatic bile ducts. Using molecular, pharmacological, and functional biophysical approaches the principal findings in these studies of mouse cholangiocytes are: (1) both small and large cholangiocytes express a repertoire of both P2X and P2Y receptors; (2) both small and large cholangiocytes develop polarized epithelial monolayers with a high transepithelial resistance and demonstrate rapid increases in $[Ca^{2+}]_i$ and transepithelial secretion (I_{sc}) upon exposure to extracellular nucleotides; (3) nucleotide-stimulated secretion is dependent on IP3 receptor-mediated increases in $[Ca^{2+}]_i$ and Ca^{2+}-activated Cl^- channel activation; (4) both small and large cholangiocytes demonstrate mechanosensitive ATP release which is dependent on intact vesicular trafficking pathways; and (5) the magnitude of mechanosensitive ATP release is significantly greater in small versus large cholangiocytes. Thus, these studies demonstrate that both small and large cholangiocytes express all components of the purinergic signaling axis and collectively, provide a working model for mechanosensitive ATP-stimulated secretion along intrahepatic bile ducts. Additionally, the ATP-mediated secretory pathway identified in the mouse small cholangiocytes, which do not exhibit secretin-stimulated secretion,[3,17] represent the first identification of a secretory pathway in these specialized cells. The existence of a gradient along the biliary axis, wherein ATP released from small cholangiocytes "upstream" may represent an important paracrine signal to the "downstream" P2 receptor-expressing large cholangiocytes, has important implications for bile formation (Fig. 8).

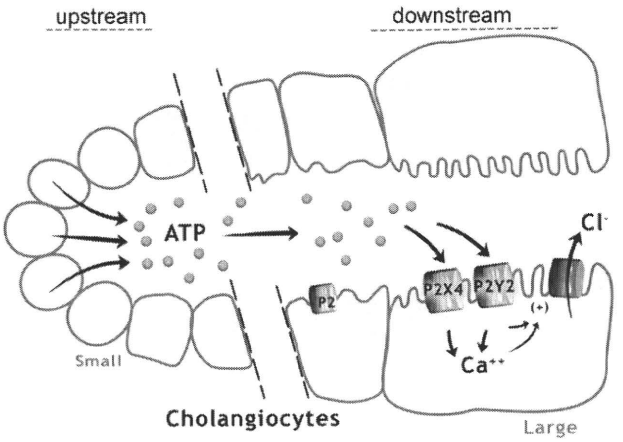

Fig. 8. Proposed model of the purinergic signaling axis along the intrahepatic bile duct. ATP released from small cholangiocytes lining the "upstream" small intrahepatic bile ducts may contribute importantly to local purinergic signaling, serve as a source for ATP in bile, and represent an important paracrine signal to the large cholangiocytes lining the larger "downstream" bile ducts. Both small and large cholangiocytes express a full array of P2 receptors and respond to extracellular nucleotides with increases in $[Ca^{2+}]_i$ and Cl^- secretion.

Although regulated ATP release has been identified in all liver cells studied, including both human and rat hepatic parenchymal cells and biliary epithelial cells,[20,22] these are the first studies to characterize ATP release in mouse cholangiocytes, and several observations deserve highlighting. First, the magnitude of ATP release from small cholangiocytes was significantly greater than that from large cholangiocytes. Because the mechanism of cholangiocyte ATP release has not been identified, the cellular basis for this difference in ATP release cannot be determined. Although CFTR has been proposed as a regulator of ATP release,[12,24,25] MSC do not express CFTR,[17] suggesting alternate ATP release pathways in these cells. One proposed alternate mechanism involves exocytosis of ATP-enriched vesicles. In fact, biliary cells possess a dense population of vesicles ~140 nm in diameter in the subapical space,[26] and increases in cell volume increase the rate of exocytosis to values sufficient to replace ~30% of plasma membrane surface area within minutes. In the current studies, stimuli associated with ATP release were also associated with parallel increases in the rate of exocytosis, and disruption of vesicular trafficking significantly decreased ATP release. Notably, overall rates of exocytosis in response to mechanosensitive stimuli did not vary significantly between MLCs and MSCs, despite a significantly greater release of ATP from MSCs, given the same stimulus. This may suggest the existence of distinct vesicle populations contributing to regulated ATP release. In fact, recent findings in rat liver cells suggest that a distinct population of ATP-enriched vesicles may contribute to regulated ATP release.[27] In some cell types, the concentration of ATP within secretory vesicles may approach 50 mM[28] and, therefore, only several vesicles per cell may account for substantial differences in the concentration of ATP released into the extracellular space. Differences observed in the magnitude of ATP release between MSCs and MLCs may be related to variation in the regulation and/or trafficking of specific vesicles involved in ATP transport (either ATP-containing

vesicles and/or vesicles transporting an ATP transporter to the membrane). This regulation may occur at the level of vesicle "priming", trafficking, or membrane fusion/release, though clearly further work is required. Nonetheless, if these observations apply to *in vivo* conditions, greater ATP release from small cholangiocytes would translate into a significant increase in the concentration of ATP in bile in the "upstream" intrahepatic ducts, given their smaller cross-sectional area and relative volume.[29]

Second, it is notable that extracellular nucleotides elicit secretory responses when applied at both apical and basolateral membranes. The apical membrane specifically represents an anatomic orientation that is well suited for hepatocyte-to-cholangiocyte or cholangiocyte-to-cholangiocyte signaling by release of ATP into bile. This is notably distinct from secretin and other hormones that are delivered to the basolateral membrane through the bloodstream.[1] ATP release from the hepatocyte canalicular membrane may signal to downstream small and large cholangiocytes through apical P2 receptor stimulation in a process known as hepatobiliary coupling. Hepatobiliary coupling has also been described for bile acids, which are released from the hepatocyte canalicular membrane and may be transported into "downstream" cholangiocytes via the apical Na^+-dependent bile acid transporter located on large, but not small, cholangiocytes.[30] Interestingly, Ursodeoxycholic acid is associated with cholangiocyte ATP release and Cl^- secretion.[24] Thus, the ductal concentration of ATP appears to be an important determinant of bile formation and may represent a final common pathway in coupling hepatocyte transport to cholangiocyte secretion.

Lastly, the relative importance of secretin- versus P2 receptor-mediated secretion, in bile formation is unknown. The molecular identity of the Cl^- channel(s) activated in response to ATP remains undefined in biliary epithelium, though it appears to be unrelated to CFTR.[10] Furthermore, although we have previously identified the Ca^{2+}-activated K^+ channels, SK2 and IK-1, in rat and human biliary epithelial cells,[7,8] the expression and contribution of these channels to secretion in mouse cholangiocytes has not been defined.

In conclusion, the present studies represent a functional characterization of the purinergic signaling axis in mouse cholangiocytes from distinct areas of the intrahepatic biliary tree. The findings support a model wherein ATP released from small cholangiocytes lining the "upstream" small intrahepatic bile ducts may contribute importantly to local purinergic signaling, serve as a source for ATP in bile, and represent an important paracrine signal to the large cholangiocytes lining the larger "downstream" bile ducts. Targeting P2 receptor-mediated signaling pathways in intrahepatic biliary epithelial cells may provide new and innovative strategies for stimulating bile formation in the treatment of cholestatic liver diseases.

References

1. Fitz JG. Cellular mechanisms of bile secretion. In: Zakim D, Boyer TD, eds. Hepatology. ed 3. Philadelphia: W.B. Saunders Co.; 1996:362-376.
2. Alpini G, Roberts S, Kuntz SM, Ueno Y, Gubba S, Podila PV, et al. Morphological, molecular, and functional heterogeneity of cholangiocytes from normal rat liver. Gastroenterology 1996;110:1636-1643.
3. Francis H, Glaser S, Demorrow S, Gaudio E, Ueno Y, Venter J, et al. Small mouse cholangiocytes proliferate in response to H1 histamine receptor stimulation by activation of the IP3/CaMK I/CREB pathway. Am J Physiol Cell Physiol 2008;295:C499-C513.
4. Ueno Y, Alpini G, Yahagi K, Kanno N, Moritoki Y, Fukushima K, et al. Evaluation of differential gene expression by microarray analysis in small and large cholangiocytes isolated from normal mice. Liver Int 2003;23:449-459.
5. Martinez-Anso E, Castillo JE, Diez J, Medina JF, Prieto J. Immunohistochemical detection of chloride/bicarbonate anion exchangers in human liver. HEPATOLOGY 1994;19:1400-1406.
6. Chari RS, Schutz SM, Haebig JA, Shimokura GH, Cotton PB, Fitz JG, et al. Adenosine nucleotides in bile. Am J Physiol 1996;270: G246-G252.
7. Feranchak AP, Doctor RB, Troetsch M, Brookman K, Johnson SM, Fitz JG. Calcium-dependent regulation of secretion in biliary epithelial cells: the role of apamin-sensitive SK channels. Gastroenterology 2004; 127:903-913.
8. Dutta AK, Khimji AK, Sathe M, Kresge C, Parameswara V, Esser V, et al. Identification and functional characterization of the intermediate conductance Ca2+-activated K+ channel (IK-1) in biliary epithelium. Am J Physiol Gastrointest Liver Physiol 2009;297:G1009-G1018.
9. McGill J, Basavappa S, Shimokura GH, Middleton JP, Fitz JG. Adenosine triphosphate activates ion permeabilities in biliary epithelial cells. Gastroenterology 1994;107:236-243.
10. Dutta AK, Woo K, Doctor RB, Fitz JG, Feranchak AP. Extracellular nucleotides stimulate Cl- currents in biliary epithelia through receptor-mediated IP3 and Ca2+ release. Am J Physiol Gastrointest Liver Physiol 2008;295:G1004-G1015.
11. Schlenker T, Romac JMJ, Sharara A, Roman RM, Kim S, LaRusso N, et al. Regulation of biliary secretion through apical purinergic receptors in cultured rat cholangiocytes. Am J Physiol 1997;273:G1108-G1117.
12. Minagawa N, Nagata J, Shibao K, Masyuk AI, Gomes DA, Rodrigues MA, et al. Cyclic AMP regulates bicarbonate secretion in cholangiocytes through release of ATP into bile. Gastroenterology 2007;133: 1592-1602.
13. Woo K, Dutta AK, Patel V, Kresge C, Feranchak AP. Fluid flow induces mechanosensitive ATP release, calcium signalling and Cl- transport in biliary epithelial cells through a PKCzeta-dependent pathway. J Physiol 2008;586:2779-2798.
14. Dranoff JA, Masyuk AI, Kruglov EA, LaRusso NF, Nathanson MH. Polarized expression and function of P2Y ATP receptors in rat bile duct epithelia. Am J Physiol Gastrointest Liver Physiol 2001;281: G1059-G1067.
15. Doctor RB, Matzakos T, McWilliams R, Johnson S, Feranchak AP, Fitz JG. Purinergic regulation of cholangiocyte secretion: identification of a novel role for P2X receptors. Am J Physiol Gastrointest Liver Physiol 2005;288:G779-G786.
16. Ishii M, Vroman B, LaRusso N. Isolation and morphologic characterization of bile duct epithelial cells from normal rat liver. Gastroenterology 1989;97:1236-1247.

17. Glaser SS, Gaudio E, Rao A, Pierce LM, Onori P, Franchitto A, et al. Morphological and functional heterogeneity of the mouse intrahepatic biliary epithelium. Lab Invest 2009;89:456-469.
18. Gatof D, Kilic G, Fitz JG. Vesicular exocytosis contributes to volume-sensitive ATP release in biliary cells. Am J Physiol Gastrointest Liver Physiol 2004;286:G538-G546.
19. Taylor AL, Kudlow BA, Marrs KL, Gruenert D, Guggino WB, Schwiebert EM. Bioluminescence detection of ATP release mechanisms in epithelia. Am J Physiol 1998;275:C1391-C1406.
20. Feranchak AP, Fitz JG, Roman RM. Volume-sensitive purinergic signaling in human hepatocytes. J Hepatol 2000;33:174-182.
21. Salter KD, Fitz JG, Roman RM. Domain-specific purinergic signaling in polarized rat cholangiocytes. Am J Physiol Gastrointest Liver Physiol 2000;278:G492-G500.
22. Feranchak AP, Roman RM, Doctor RB, Salter KD, Toker A, Fitz JG. The lipid products of phosphoinositide 3-kinase contribute to regulation of cholangiocyte ATP and chloride transport. J Biol Chem 1999; 274:30979-30986.
23. Dubyak GR, El-Moatassim C. Signal transduction via P2-purinergic receptors for extracellular ATP and other nucleotides. Am J Physiol 1993;265:C577-C606.
24. Fiorotto R, Spirli C, Fabris L, Cadamuro M, Okolicsanyi L, Strazzabosco M. Ursodeoxycholic acid stimulates cholangiocyte fluid secretion in mice via CFTR-dependent ATP secretion. Gastroenterology 2007;133: 1603-1613.
25. Braunstein GM, Roman RM, Clancy JP, Kudlow BA, Taylor AL, Shylonsky VG, et al. Cystic fibrosis transmembrane conductance regulator facilitates ATP release by stimulating a separate ATP release channel for autocrine control of cell volume regulation. J Biol Chem 2001;276:6621-6630.
26. Doctor RB, Dahl R, Fouassier L, Kilic G, Fitz JG. Cholangiocytes exhibit dynamic, actin-dependent apical membrane turnover. Am J Physiol Cell Physiol 2002;282:C1042-C1052.
27. Feranchak AP, Lewis MA, Kresge C, Sathe M, Bugde A, Luby-Phelps K, et al. Initiation of purinergic signaling by exocytosis of ATP-containing vesicles in liver epithelium. J Biol Chem 2010;285:8138-8147.
28. Bergendorff A, Uvnas B. Storage properties of rat mast cell granules in vitro. Acta Physiol Scand 1973;87:213-222.
29. Masyuk TV, Masyuk AI, Ritman EL, LaRusso NF. Three-dimensional reconstruction of the rat intrahepatic biliary tree: physiologic implications. In: Alpini G, Alvaro D, Marzioni M, Lesage G, LaRusso N, eds. The Pathophysiology of Biliary Epithelia. Georgetown, TX: Landes Bioscience; 2004:60-71.
30. Alpini G, Glaser SS, Rodgers R, Phinizy JL, Robertson WE, Lasater J, et al. Functional expression of the apical Na+-dependent bile acid transporter in large but not small rat cholangiocytes. Gastroenterology 1997;113:1734-1740.

Hepatology Research

Hepatology Research 2010; **40**: 1219–1226 doi: 10.1111/j.1872-034X.2010.00727.x

Original Article

Cyclooxygenase-2 gene promoter polymorphisms affect susceptibility to hepatitis C virus infection and disease progression

Masashi Sakaki,[1] Reiko Makino,[1,2] Kazumasa Hiroishi,[1] Kumiko Ueda,[2] Junichi Eguchi,[1] Ayako Hiraide,[1] Hiroyoshi Doi,[1] Risa Omori[1] and Michio Imawari[1]

[1]*Division of Gastroenterology, Department of Medicine,* [2]*Clinical Research Laboratory, Showa University School of Medicine, Tokyo, Japan*

Aim: Because polymorphisms of cyclooxygenase-2 (*COX-2*) and osteopontin (*OPN*) promoter regions and a promoter/enhancer region of forkhead box protein 3 (*FOXP3*) gene are known to affect immune responses, we examined whether these polymorphisms can influence susceptibility to hepatitis C virus (HCV) infection and progression of liver disease.

Methods: Peripheral blood samples were obtained from 104 Japanese patients with chronic HCV infection and 74 healthy Japanese donors. Polymerase chain reaction single-stranded conformational polymorphism analysis of genomic DNA was performed to determine the polymorphisms.

Results: The risk of persistent HCV infection was decreased in subjects with –1195GG genotype of the *COX-2* promoter region. However, in patients with chronic HCV infection, the –1195GG genotype was associated with advanced-stage liver disease. A luciferase reporter assay performed to analyze the effect of single nucleotide polymorphisms (SNP) (–1195A or –1195G) in *COX-2* gene on transcriptional activity using the HepG2, Huh7 and HeLa cell lines indicated that the –1195G genotype showed higher transcriptional activity than the –1195A genotype. SNP of *OPN* and *FOXP3* did not differ between patients with chronic HCV infection and controls. However, the –443TT genotype of the *OPN* promoter region was associated with increased inflammatory activity of the liver.

Conclusion: These results suggest that the –1195GG genotype of the *COX-2* promoter region protects against HCV infection in the Japanese. However, once chronic infection is established, the –443TT genotype of the *OPN* promoter region and the –1195GG genotype of the *COX-2* promoter are thought to promote inflammation and contribute to the progression of liver disease.

Key words: cyclooxygenase-2, forkhead box protein 3, hepatitis C virus, osteopontin, single nucleotide polymorphisms

INTRODUCTION

HEPATITIS C VIRUS (HCV) infection causes chronic hepatitis (CH), liver cirrhosis (LC) and eventually leads to hepatocellular carcinoma (HCC). Immune responses are thought to play important roles in the pathogenesis of viral hepatitis and inflammation is thought to be an important factor in the progression of liver injury.

Cyclooxygenase-1 (COX-1) and COX-2 are enzymes that convert arachidonic acid into prostaglandins and thromboxanes. COX-1 is constitutively expressed in various tissues and plays important roles in homeostasis. In contrast, COX-2 is involved in inflammation, angiogenesis, anti-apoptosis and carcinogenesis.[1–4] COX-2 has been reported to be overexpressed in inflammatory tissues and cancers.[5–8]

The HCV core, NS3 and NS5A proteins are shown to stimulate COX-2 expression.[9,10] Overexpression of COX-2 has been reported in CH, LC and HCC tissues. Furthermore, the COX-2 expression level has been reported to correlate with HCV liver injury activity and

Correspondence: Professor Michio Imawari, Division of Gastroenterology, Department of Medicine, Showa University School of Medicine, 1-5-8 Hatanodai, Shinagawa-ku, Tokyo 142-8666, Japan. Email: imawari@med.showa-u.ac.jp

Received 25 July 2010; revision 3 August 2010; accepted 9 August 2010.